TSINGHUA UNIVERSITY

FINAL DEGREE PROJECT

A communication-based algorithm to avoid the human body effect on antennas

Student: Javier Martinez Garcia
Supervisor: Zhijun Zhang
Telecommunications Engineering
Department of Electronic Engineering
Tsinghua University
22/06/2011

Abstract

In the mobile communications field there are many studies about the negative effects that a human operator can cause on the antenna when interacting with a mobile device. Basically, these effects are body absorption and impedance mismatching and both involve loss of radiated power. The current reduced size of these types of terminals makes the influence more severe, thus deteriorating the quality of the global service.

This project deals with the problem of the variation of the antenna impedance due to human proximity and proposes a system which is able to minimize the losses by correcting the operating frequency of the communication between a base station and a mobile terminal. For this purpose, once studied all the initial conditions, which included an analysis of the frequency band utilized (around 400 MHz) and the already fabricated mobile terminal whose antenna was a PIFA, the designing stage was started. This stage contemplated two typical approaches in the antenna design: firstly, in a purely physical approach, the antenna for the base station was designed and manufactured; secondly, a logic level approach which consisted of the development of an algorithm and its implementation on the System-on-Chip that each device incorporated together with the corresponding antenna. All the considerations made at this stage fulfilled specific requirements, like timing, power or frequency requirements.

After verifying the system performance, a set of experiments was carried out to determine if the goal of the project was achieved. It was obtained power increments between 3 and 11 dB depending on the relative distance of the influent body, always displacing the operating frequency to a lower one. A 600 ms time response was correctly tested and it was possible to increase it if more frequency precision was needed. In addition, a maximum range of 300 m using the higher power available in the devices was predicted but not tested. To finish, some improvements based on the introduction of data packets in the communication algorithm were examined and commented.

Contents

Index of figures

Index of tables

1. Introduction

1.1. Antennas for mobile communications: a brief overview

During the first half of the XX century, the necessity of advanced antenna designs arose. However, it was from the 1960s and mainly from the 1990s when a revolutionary progress in integrated circuits and information science allowed engineers to develop new kinds of antennas. These novel designs supposed a radical change compared with the previous ones: antennas became less bulky, lightweight, low cost, easy to manufacture, less power-consuming and compatible with the recently appeared electronic devices. Antennas were ready, then, to face the demands of the mobile communications market.

Nowadays, one has to consider the following tendencies when is planning to start a design of an antenna:

- Personalization. Depending on which is the goal of the terminal the features of the antenna may vary. It is not the same the design of an antenna for a mobile phone, which currently provides many extra functions, to the design of an antenna for very short ranges, like those that are integrated in devices for control and identification. The second one has more relaxed electromagnetic specifications (e.g. no high gain) that will permit, for instance, to reduce the volume of the antenna even more.
- Globalization. Different types of services (such as 2G, 3G, GPS, Wi-Fi, Bluetooth…) should be able to be rendered by mobile terminals. Each service may work in different band, hence antennas have to be multiband, that is antennas that can perform well in two, three, four or even five bands.
- Multimedia services. Current mobile systems not only cover voice service, but also data services (internet, music, video…). In order to ensure high data rates which can carry all this information it is extremely necessary to introduce the latest technologies in the field of antennas and signal processing, such as adaptive arrays, transmission and reception of diversity, and wideband, multiband and MIMO antennas.
- Software implementation. This trend has a lot to do with the present project. Trough software which controls the antenna, the performance will be improved. For instance, adaptive control of the antenna can change the features (power, radiation pattern, bandwidth, impedance…) depending on the environmental conditions. In this project, a program that corrects the detuning of the antenna due to the human body effect will be implemented. More details will be given later.

In addition, engineers will find some limitations that are derived directly from the aforementioned trends. One of them is downsizing of the whole device. The fact is that clients demand quite small terminals because they are easy to carry, but, on the other hand, clients want all the newest functions kept. Therefore, antenna designers only dispose of limited space to place the antenna. Moreover, since the device must be compact, all the components which are inside it should be arranged close to each other, so that the antenna performance (e.g. power radiated) is affected by the presence of these components. Engineers must pay special attention to those effects when designing and take the antenna not as an isolated piece, but as a set of pieces that must work together.

Another consequence of the limited antenna size is that it is not possible to have large bandwidth and efficiency at the same time. This is because there is a relationship between the antenna dimensions, the bandwidth and the efficiency when the antenna is small compared with the working wavelength. It is shown in the following well-known expression for small antennas:

$$BW \cdot \eta \cong (ka)^3 \quad (\text{if } ka \ll 1)$$

where *BW* is the antenna bandwidth, η is the antenna efficiency, k is the wave number and a is the diameter of the equivalent antenna volume. The equation means that once the dimensions and the operating frequency are fixed, if more bandwidth is desired, losses will have to be allowed in order to reduce the efficiency.

Besides the size of the antenna, the ground plane extension and the terminal shape play an important role in the antenna performance because, actually, they belong to the whole radiating element. The ground plane size affects directly to the operating frequency, the impedance matching, the bandwidth, the radiation pattern and the interaction with the user.

After, having summarized very briefly some of the most significant and general concepts in the current state of art, the designs that are being deployed currently in mobile handsets and similar devices are going to be presented.

The first antenna designs were external, that is the antenna element was placed outside the terminal, commonly mounted on the top of it. One very usual example is the whip antenna (see *Figure* 1) which consists of a $\lambda/4$ monopole mounted on the handset surface, which acts as ground plane. Whip antennas provide omnidirectional patterns and are easy to fabricate. The problem that they are too long at low frequency bands can be solved by bending the wire to make a helix so the structure becomes shorter. Engineers also created dual band helix antennas in which the second resonance is controlled by a non-uniform pitch angle or diameter. Many other variations and combinations can be found.

Figure 1: Whip antenna with a stubby element

As it has been commented above, antenna downsizing is a challenge for engineers. A way of making smaller terminals, and also more comfortable and practical for the user, was inserting the antenna into the device, so that the antenna became internal. These kinds of antennas are constructed on the main Printed Circuit Board (PCB) of the mobile set. The first design was a modification of a monopole which had a form of T or inverted-L (Inverted-L Antenna or ILA). Afterwards, it was introduced a tuning element into the ILA creating the IFA (Inverted-F Antenna). The next step was the transformation the antenna element form a wire to a plate in order to achieve broad bandwidth characteristics. This

last kind of antenna is known as Planar Inverted-F Antenna (PIFA). In *Figure 2*, the differences between monopole, ILA, IFA and PIFA are shown in a simple manner.

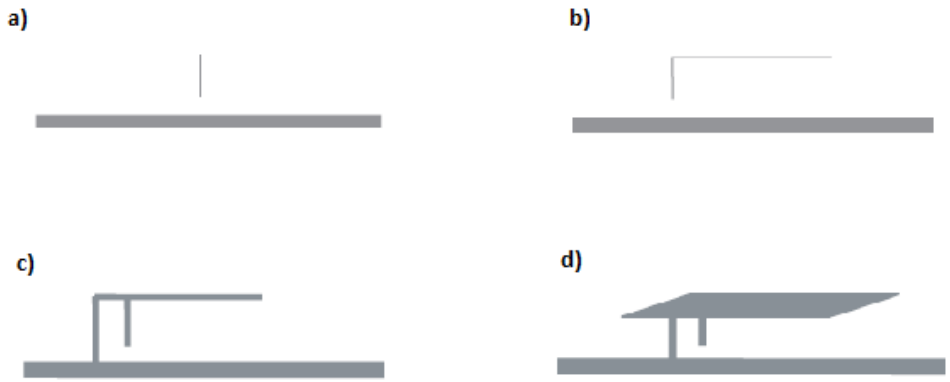

Figure 2: (a) Monopole, (b) ILA, (c) IFA, (d) PIFA

PIFAs are widely used in the current mobile terminals as well as printed loops and monopoles antennas. A few pictures of these types of antennas can be seen in *Figure 3* .

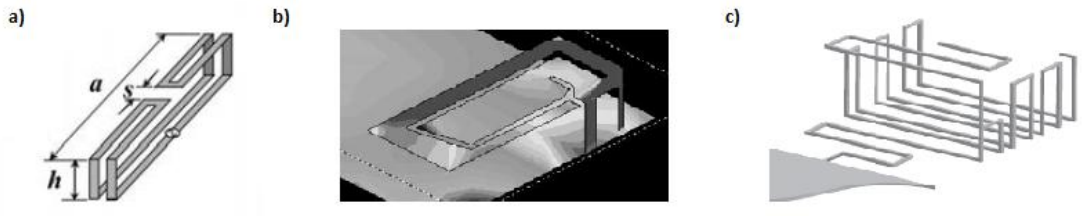

Figure 3: (a) Folded Loop, (b) PIFA, (c) 3D folded and branched monopole

In many cases, the structuring elements are folded in the three dimensions of the space, as is also seen in two designs of *Figure 3*, to obtain better performance and use all the volume available. Apart from the total length of the antenna, other elements, such as stubs or dielectrics, can help engineers to reach the design which has the optimal performance and cover all the desired bands. To finish, the use of multiple antennas and MIMO schemes exploit multipath transmission, thus getting higher data rates.

1.2. The human body effect on antenna performance

1.2.1. Useful background concepts

Before focusing on the effects of the proximity of humans on the antenna, it is convenient to revise some concepts about impedance matching. It is well known that a good impedance matching within a certain bandwidth is required to avoid losing too much radiated power and, hence, too much efficiency. The amount of power which is not radiated is either reflected to the source by the effect of the impedance mismatching or lost in the antenna conductor. First of all, let's remember what impedance matching is and remind some concepts that will be useful along this report.

Input impedance is the impedance presented by an antenna at its terminals or the ratio of the voltage to current at a pair of terminals or the ratio of the appropriate

components of the electric to magnetic fields at a point. It is demonstrated that in a circuit which is made up of a generator (with its internal complex impedance) and a complex load, the maximum transference of power towards the load is achieved when the load impedance value is the conjugated of the generator impedance value (i.e. conjugate matching). In *Figure 4* an antenna and its source are shown as well as and its Thevenin equivalent.

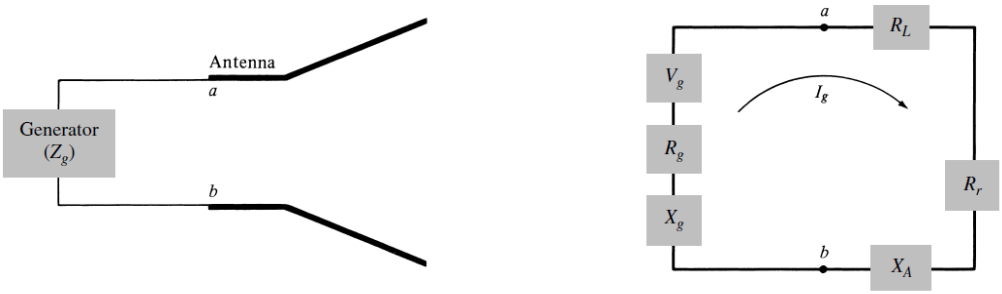

Figure 4: Antenna in transmitting/receiving mode (left) and Thevenin equivalent circuit (right)

Notice that the impedance of the generator is $Z_g = R_g + jX_g$ and the antenna impedance is $Z_A = R_A + jX_A = (R_L + R_r) + jX_A$. Then, the conjugate matching occurs when $Z_A = Z_g^*$. The real part of the antenna impedance can be divided into loss resistance, in which the power is lost because of the heating of the conductor, and radiation resistance, through which the power is radiated towards the space. As a consequence, it would be desired a high radiation resistance compared to the loss resistance. The parameter that weights this relationship is the antenna radiation efficiency η_{rad}:

$$\eta_{rad} = \frac{R_r}{R_r + R_L} = \frac{P_{radiated}}{P_{accepted}}$$

where R_r is the radiation resistance, R_L is the loss resistance, $P_{radiated}$ is the power radiated towards the space and $P_{accepted}$ is all the power that is not reflected towards the source.

The radiation efficiency also relates the gain (G) and the directivity (D) of an antenna:

$$G = \eta_{rad} \cdot D$$

In a perfect and unfeasible situation, there is no loss resistance, so the efficiency will be equal to 1 and the gain will coincide with the directivity. By contrast, if the losses in the antenna are high, the radiation efficiency will be poor. Nowadays, efficiency, together with return losses, is a parameter of vital importance since most of terminals need a battery, which has a limited duration.

As it has been mentioned above, return loss (i.e. power reflected to the source) has to be considered when designing an antenna. It must be limited the power reflected not only because is power that is not radiated towards the space, but also because is power that can damage power amplifiers in the transmitting mode of the antenna. There are

some indicators that help us to measure and understand this kind of loss and to determine when there is a mismatching situation. Some of them are the complex reflection coefficient (1), the return loss indicator (2), the mismatch loss indicator (3) and the *VSWR* (4) (Voltage Standing Wave Ratio). In the following lines, they are expressed mathematically, respectively:

$$\Gamma_A = \frac{Z_A - Z_o}{Z_A + Z_o} = S_{11} \qquad (1)$$

$$RL(\text{dB}) = 10\log\left(\frac{P_{incident}}{P_{reflected}}\right) = -10\log|\Gamma_A|^2 \qquad (2)$$

$$ML(\text{dB}) = 10\log\left(\frac{P_{incident}}{P_{accepted}}\right) = -10\log(1-|\Gamma_A|^2) \qquad (3)$$

$$VSWR = \frac{V_{MAX}}{V_{MIN}} = \frac{1+|\Gamma_A|}{1-|\Gamma_A|} \qquad (4)$$

In this report, it will be used the reflection coefficient either in the complex form or in dB, even though all the indicators express the same in different ways. On one hand, the complex reflection coefficient measures the matching with respect to the reference impedance (usually $Z_o = Z_g$, being Z_o the reference impedance). On the other hand, for instance, *VSWR* is related to the amplitude of the stationary wave in the equivalent transmission line. Note that the reflection coefficient contains phase information, which is basic when calculating the necessary elements for matching the antenna impedance to the source, whereas *VSWR* only takes into account the modulus information. In the present document, the reference to the modulus of the reflection coefficient, if it is not said the contrary, will be denoted simply as S_{11}.

It is worth also commenting that there is another efficiency parameter concerning the mismatching losses, which is the reflection efficiency η_{refl}. It measures the ratio between the power accepted by the antenna and the incident power. Not all the incident power will be accepted by the antenna, hence:

$$\eta_{refl} = \frac{1}{ML} = \frac{P_{accepted}}{P_{incident}} = 1-|\Gamma_A|^2$$

If the reflection and the radiation efficiency are combined, it is obtained the total efficiency. Total efficiency is useful when the matching conditions are not good, that is the operating frequency is not the optimal (explanation later). It is defined as:

$$\eta_{total} = \eta_{rad} \cdot \eta_{refl}$$

Similarly to the gain, realized gain can be obtained if total efficiency is known. The realized gain ($G_{realized}$) is a good indicator of the antenna gain over different frequencies because not only takes into account the radiation losses (that may be almost constant within the considered bandwidth), but also the reflected power (that a priori will suffer stronger effects for different operating frequencies). Consequently, in general, the realized gain will be lower than the gain. It is defined as follows:

$$G_{realized} = \eta_{rad} \cdot \eta_{refl} \cdot D = \eta_{total} \cdot D = \eta_{refl} \cdot G$$

Since the input impedance of an antenna is a function of frequency, both reflection coefficient and *VSWR* are measured with respect to frequency. Around the optimal frequency point reflection coefficient will tend to 0 whereas *VSWR* will be almost 1 (from here, this point will be sometimes referred, in a non-exact way, as resonant frequency or center frequency). In this project, frequencies in which reflection coefficient is below -6 dB or *VSWR* is below 3 will be considered inside the antenna impedance bandwidth and, therefore, the matching conditions will be fulfilled. In *Figure 5*, it can be seen the reflection coefficient (dB) of a penta-band antenna. The frequency points where the reflection coefficient is minimum and those that are near these minimums belong to the frequency bands where the antenna may work. It is worth noting that the design which provides the optimum reflection coefficient or *VSWR* may not provide the optimum efficiency of the antenna.

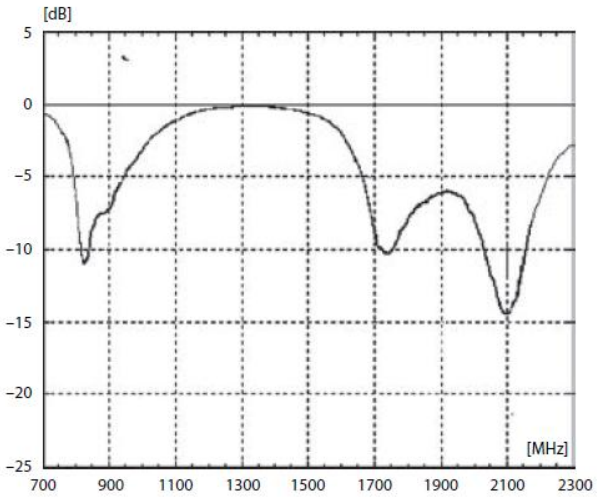

Figure 5: Example of the reflection coefficient of a penta-band antenna

The next step after designing all the factors that will determine the antenna impedance (like its geometry, its method of excitation or its proximity to surrounding elements) is to improve the impedance matching within the aforementioned bandwidth, if necessary. The group of elements which constitutes the matching network can include inductors, capacitors and other elements. Inductors and capacitors are constructed with concentrated elements, when the operating frequency is low, or with transmission lines, when working with microwaves.

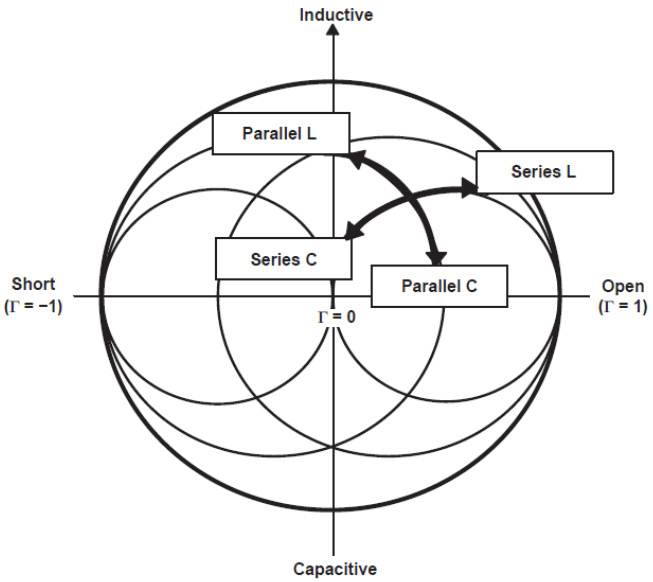

Figure 6: Effects of capacitors C and inductors L on the antenna impedance

A commonly used tool to design matching networks is the Smith Chart. It plots the reflection coefficient (its module and phase) and, hence, the antenna impedance in the complex plane. If these magnitudes are plotted versus the frequency, one can see curved lines on the graphic. *Figure 6* exhibits the effect of single capacitors and inductors (in series and shunt configurations) on the antenna impedance, which consists of moving the reflection coefficient over the complex plane. In the case of impedance matching, which is the present case, it would be desired to move this coefficient to the center of the Smith Chart where the reflection coefficient is close to 0.

1.2.2. Human body effects and possible solutions

In the real situations the antenna is not isolated: firstly, it is surrounded by the elements that provide additional functions to the mobile terminal in a quite reduced volume. These devices are taken into account by engineers when they are designing the terminal because of their effects on the antenna performance, such as detuning (change of the antenna impedance, thus mismatching) or efficiency decreasing. Another element, which may influence on the antenna behavior, is the person who is operating the mobile terminal. This influence will be studied in the present project. Many publications have investigated the human body effect on antennas (for example, **[1-5]**). Reading them, one can conclude that the degradations are caused mostly by the operator's hand and head. Furthermore, there are different factors (e.g. position, distance, band, type of antenna) that determine their intensity.

Degradations are mainly classified into two kinds: the increasing of the power absorption and the increasing of the impedance mismatching. The intensity of both depends on the type of the antenna, the frequency band and the way the user hold the terminal. The investigations referenced before show that there is a total loss of 3 to 10 dB in the power radiated due to a combination of detuning and absorption. As a result, the user may notice a decrease in battery life, a deterioration of the link budget and communication quality and a rise of the number of dropped connections.

When a human body is close to an antenna, part of the power radiated towards the space is absorbed by the biological tissues of the body, thus reducing the antenna efficiency. The parameter which allows measuring how much power is absorbed when the body is exposed to electromagnetic radiation is the Specific Absorption Rate (*SAR*). *SAR* can be calculated from the electric field within a tissue as follows:

$$SAR = \frac{\sigma}{\rho}|E|^2 \quad [\frac{W}{kg}]$$

where σ is the conductivity of the body, ρ is the density of it and E is the electric field (which depends on the relative permittivity ϵ_r of the tissue at a certain frequency). *SAR* is measured directly using people or phantoms (see *Figure 7*) placed next to the mobile device in the appropriate place (e.g. anechoic chambers). Furthermore, *SAR* can be obtained using simulations based on numerical methods, such as Finite-Difference Time-Domain (FDTD) or Finite Element Method (FEM). Even though this project is not going to deal directly with SAR, it is interesting to know that there are techniques to reduce *SAR*. One of them could be to concentrate the radiated power in the opposite direction to the body, thus avoiding losing too much power by absorption.

Figure 7: Phantom for SAR measurement

The second consequence of the proximity of a person to an antenna (i.e. detuning) will be analyzed in detail. In addition, some existent solutions for such a negative effect will be exposed. As it is going to be seen later, the actual goal of this project is to design an algorithm that has to be able to avoid, in part, the problem in question.

In the previous pages, it has been explained why is important to have a good impedance matching. The presence of a person operating a mobile terminal changes the antenna input impedance, so that the antenna is not matched anymore. *Figure 8* shows how the reflection coefficient is moved towards a lower frequency band by the effect of hand's user. The way the antenna impedance varies has been also investigated. For example, a recent paper about these variations for a dual-band PIFA **[5]** concludes that "the antenna becomes more resistive and inductive as the level of user interaction increases". It also says that "knowledge of these variations can be utilized to facilitate the design of simpler, cheaper adaptive matching circuits". At the practice stage of this project, this last affirmation will be applied.

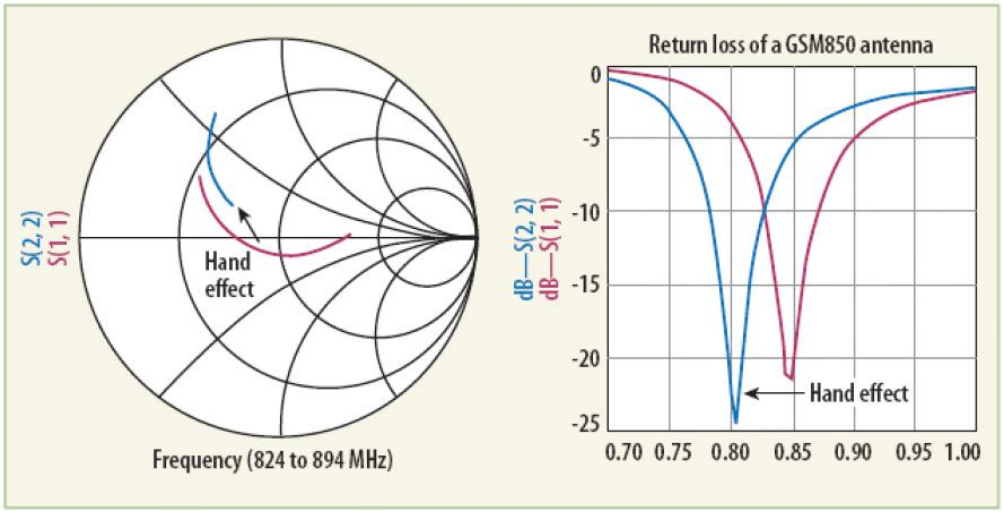

Figure 8: Example of the effect of the hand proximity on the antenna input impedance

Avoiding the detuning effect can be achieved by implementing methods based on different principles. For instance, if more than one antenna can be mounted on the mobile terminal, a diversity technique could be implemented in order to mitigate the problem of the power lost due to the mismatching. Another example is to install a hinged dielectric cover to the mobile terminal in order to keep electromagnetic sources physically away from the human body. Finally, more specific solutions for the mismatching problem are commonly used. They consist of adaptive matching networks that are able to change their impedance quickly to provide a more suitable impedance matching situation for the antenna **[6-8]**. These circuits are integrated into the antenna design, so that the whole set is known as Adaptively Tunable Antenna.

Adaptive matching networks can match again the antenna when the user proximity produces a change in the antenna impedance. In a reasonable time the impedance which the source sees becomes close to the one that it would see in case there had not been user interaction. For that purpose, it is required that the elements belonging to the matching circuit can change their value. Several technologies have been suggested as antenna tuning solutions, like Micro Electro Mechanical System (MEMS) switched capacitors or Barium Strontium Titanate (BST) capacitors. Both are variable capacitors, also known as varactors. Since it is complicated to construct variable inductors, two J-inverters and a variable capacitor could be used to simulate it. As shown in *Figure 9,* basic and well studied network configurations, such as pi networks, may be used to construct the entire network.

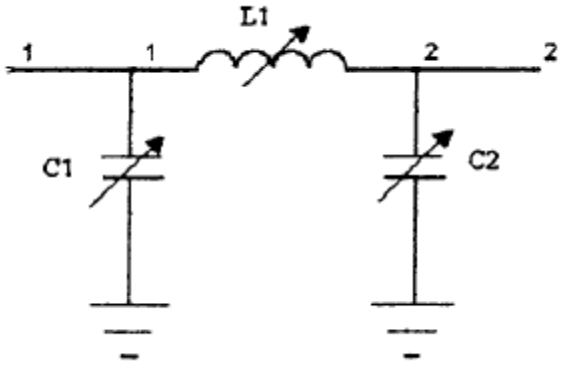

Figure 9: Basic configuration to implement the adaptive matching network

All the elements of the network should be arranged in a matrix to achieve precise control of the system impedance. Moreover, it is necessary an algorithm which controls at each moment the appropriate value of each element of the network. This algorithm is implemented on a control unit (microprocessor) that is connected to the tuner unit. In addition, a coupler is needed to decide when the matching conditions are getting worse. *Figure 10* shows a possible block diagram of the system. For more details of a complete adaptive matching system, it can be consulted **[8]**.

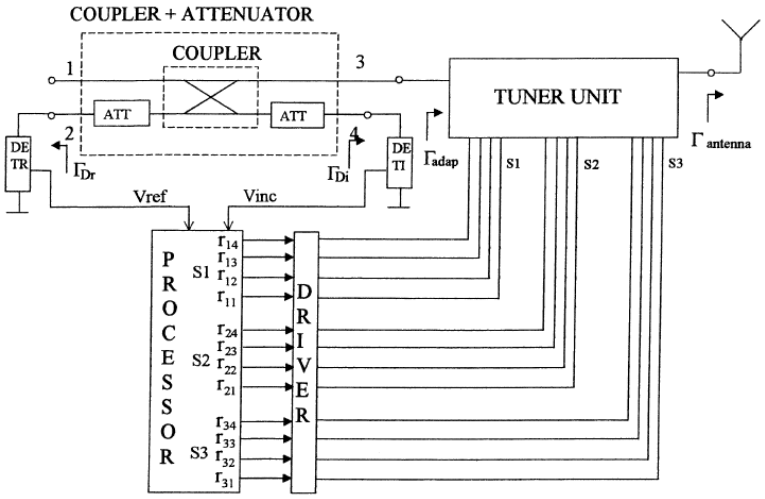

Figure 10: Block diagram of a complete automatic impedance matching system

It is worth considering a few features that are going to be required to this kind of devices. First of all, they must provide a rapid response depending on the communication protocols or the standards that are being used. For example, if the communication system requires TDD, there will be time response restrictions. Similarly, if the mobile terminal needs to work at different frequency bands at the same time (FDM), the matching network must correct the impedance matching conditions for all the bands. It is also worth noticing that even though a perfect system should cover all the Smith Chart (hence, all possible reflection coefficient values) with more or less precise steps, is not strictly necessary because the effects of the human body effect have been studied previously. From the experience one can predict which are going to be the most probable values of

the antenna impedance when the mobile handset is held in different ways. Then, the designers of the system should focus on correct these most probable values, so that the system is feasible and cheaper.

1.3. Goals and description of this report

In the following chapters, the laboratory work which has been done in the last months is going to be exposed. Firstly, it is important to delimit what is the objective of the whole project. The goal of the project is to find a quick, easy-to-implement and reliable algorithm which minimizes the human body effect on antennas. The algorithm is based on a communication protocol rather than on a system that modifies the electrical or physical properties of the antenna and the elements connected to it. Hence, the solution has not too much to do with the one that has been described before.

The system that will be proposed does not deal with adaptive matching networks, but with interaction between two devices: a base station and a mobile terminal. Basically, it consists of find out what is the best frequency to establish the communication, so the system does not correct the input impedance of the antenna. Therefore, the operating frequency will be varied while keeping the impedance characteristics that a priori have been modified by the human body influence on the antenna. The problem of the power absorbed by the body is out of the scope of the present project.

The initial point will be to describe the environment, that is the frequency band used, the System-on-Chip which provides intelligence to the antenna, and the features of the antenna of the mobile terminal. This antenna is already designed and manufactured by a workmate, so it is not a degree of freedom. On the contrary, the antenna of the base station has been designed in this project taking into account the effect of the human body on the mobile device, so its features are determined by this effect. A chapter will be dedicated to describe the design, the simulation, the fabrication and the tests of the base station antenna. Once all the elements involved in the system are presented, the report will focus on the design and implementation of the algorithm.

When designing an algorithm, it has to be considered the conditions and the scenario where the performance is going to take place. This report will include them as well as a flowchart and the description of the main functions that are derived from it. In addition, the problems and obstacles that have been appeared along the designing process and preliminary tests that have been carried out are going to be commented.

Finally, global experiments and measurements of the system for different situations (such as range or distance to the body) are going to be presented. Afterwards, some conclusions will be exposed as well as the advantages, the drawbacks and the possible improvements that could be applied.

2. Starting point: environmental considerations

2.1. Frequency band and various related aspects

2.1.1. ISM/SRD bands

The operating frequency band of the system is determined roughly by the chips which controls the antennas of the two devices (base station and mobile terminal). The chip is the CC1110, which is manufactured by Texas Instruments[1]. For this section, it is interesting to notice that the CC1110 can work in the 315/433/868/915 MHz bands. These four bands belong to the Industrial, Scientific and Medical (ISM) or Short Range Devices (SRD) bands.

ISM and SRD are the names to know a range of frequencies that have similar purposes. The difference is that the term ISM is commonly used in USA while SRD is used in EU. Both include those unlicensed bands for, usually, remote control, metering and sensing applications in short distances. It must be noted that even though these bands are license-free, it exists strict regulations (created by FCC, CEPT and ETSI[2]) which have to be respected. The limitations deal with operating frequencies, output power, spurious emissions, modulations methods, duty cycles, etc. It is important to notice that the close devices working in these bands can cause interference to another (as well as suffer it), so caution is recommended when determining the frequencies and the power levels of the system to be designed. The manufacturer of CC1110 assures in **[9]** that its transceiver chips comply with the specifications of the regulations.

2.1.2. Mobile terminal

The system which is going to be presented in this project works in the band 391 - 431 MHz, hence the bandwidth is 40 MHz. To understand why this operating frequency band is selected, the already fabricated antenna of the mobile terminal and its performance with and without a surrounding human body is going to be analyzed.

In *Figure 11* a photo of the antenna and its corresponding CC1110 System-on-Chip is shown. It can be observed that the antenna is one of the types exposed early in this document. It is a PIFA printed on a PCB designed to work around the 430 MHz band. It has a narrow impedance bandwidth and a low gain (See *Appendix A: Mobile terminal antenna parameters* for more detailed information). The criterion that was chosen was to measure the reflection coefficient modulus S_{11} first without the human body effect and,

[1] http://www.ti.com/corp/docs/aboutti.shtml

[2] FCC (Federal Communications Commission) in the USA and CEPT (Conference of Postal and Telecommunication Administration) and ETSI (European Telecommunications Standards Institute) in EU are regulatory and standardization agencies.

afterwards, in the proximity of a hand. In each case, it had to be determined which is the frequency point where the reflection coefficient is minimum (resonant frequency), that is the reflected power is minimum. Once the two points were known, the lower and upper limits of the operating bandwidth were decided.

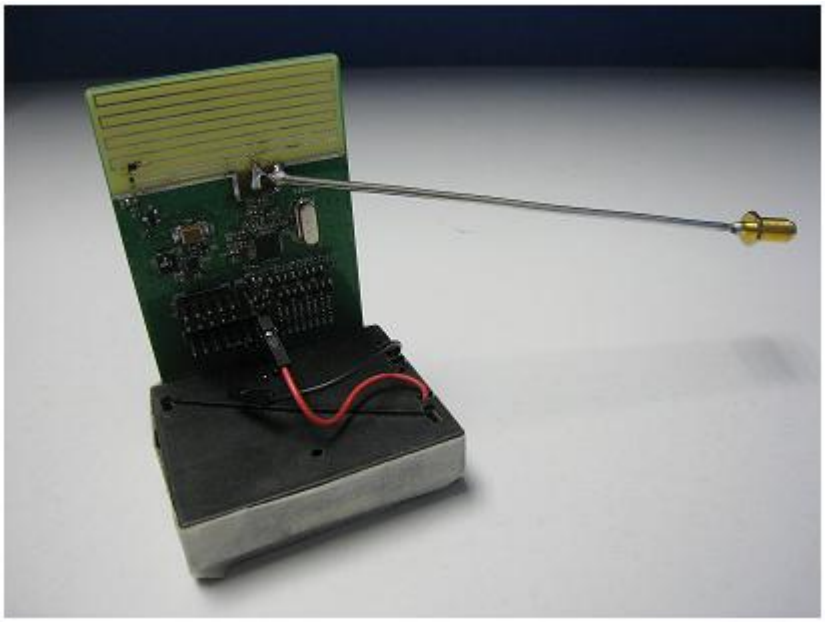

Figure 11: Photo of the mobile terminal composed of the PIFA antenna the CC1110

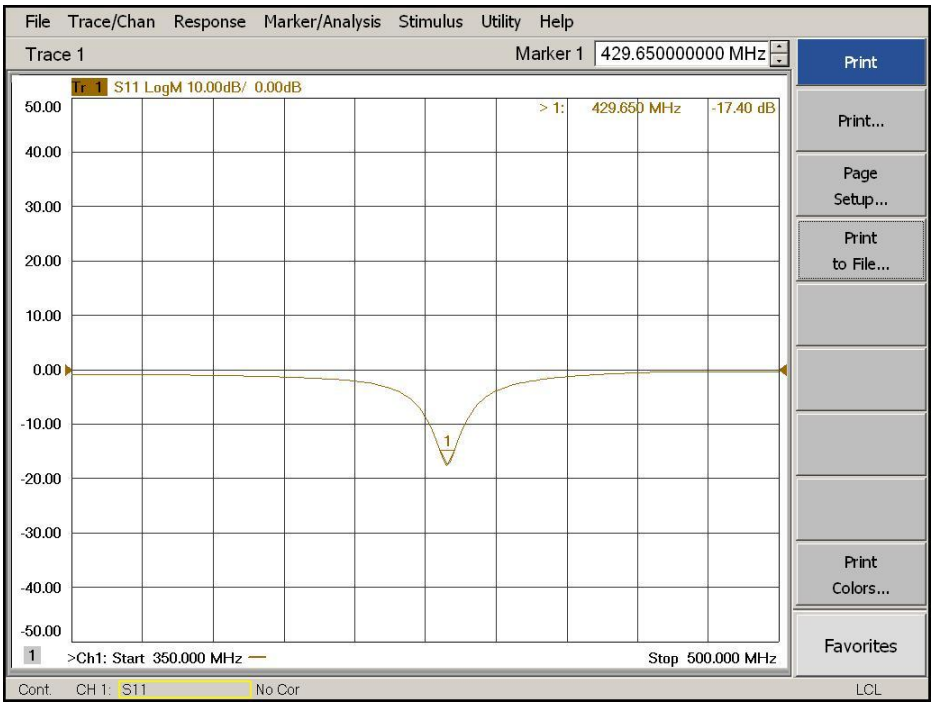

Figure 12: Reflection coefficient of the mobile terminal antenna without hand effect

The measurements were carried out with the Agilent N5247A Vector Analyzer. *Figure 12* shows the S_{11} coefficient without hand effect (isolated antenna) whereas *Figure 13*

shows the same coefficient with hand effect (about 3 mm of distance). It can be seen that the resonant frequency is displaced from 430 MHz (no hand effect) to 400 MHz (hand effect). It is also noticeable that the antenna is a narrow-band antenna, whose impedance bandwidth without the hand effect is around 15 MHz if -6 dB of reflection coefficient are considered or 7.5 MHz if are considered -10 dB. By contrast, with the presence of the hand the minimum value of the S_{11} coefficient is a bit larger and the impedance bandwidth is increased as well. Different positions of the hand were tested and always the resonant frequency became lower with more or less intensity.

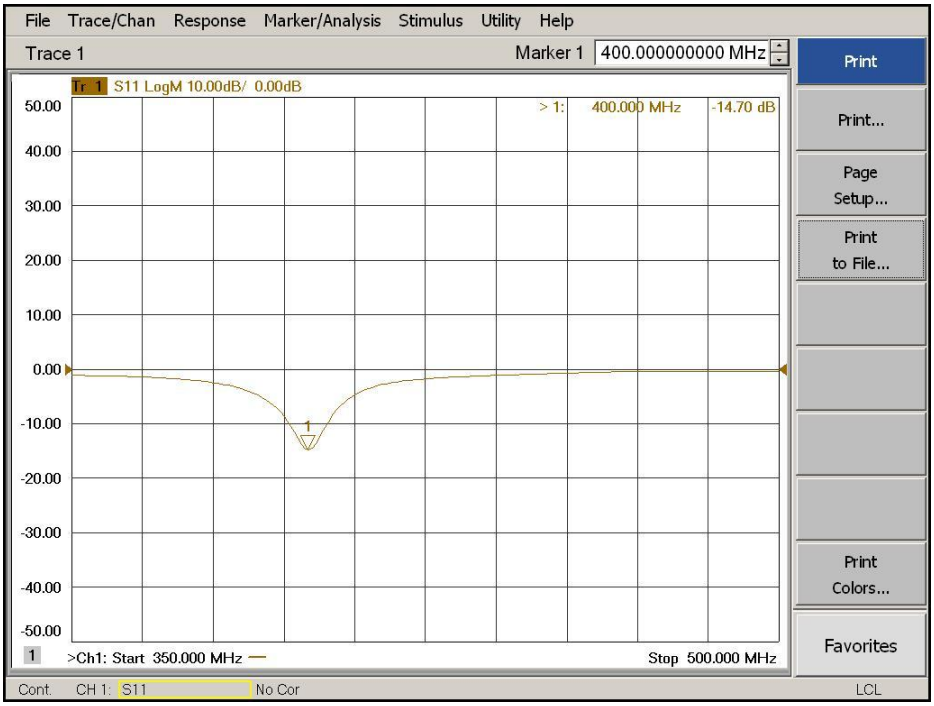

Figure 13: Reflection coefficient of the mobile terminal antenna with hand effect

Since the resonant frequency of the isolated mobile terminal is around 430 MHz, the selected upper operating frequency of the system that was being designed was 431 MHz. In the selection of the lower operating frequency was considered that the hand effect could be more severe, thus displacing even more the resonance frequency to lower bands. Therefore, the lowest possible operating frequency imposed by the CC1110 chip was chosen, that is 391 MHz. The working bandwidth was then set to 391 - 431 MHz, hence the antenna for the base station had to cover this bandwidth. The design and fabrication of this antenna is going to be shown later. Now it is time to know what the features of the CC1110 chip are and how they can be applied.

2.2. The CC1110 System-on-Chip

To provide intelligence to both base station and mobile terminal antennas, it is necessary to connect them to an integrated chip where a software application can be implemented. In this project, the aforementioned CC1110 of Texas Instruments is employed. If it is wanted to have complete information about the CC1110, is worth reading its datasheet **[10]**. Some important features which have to be taken into account

in order to design the system are listed below. In addition, *Figure 14* shows the whole diagram block of CC1110.

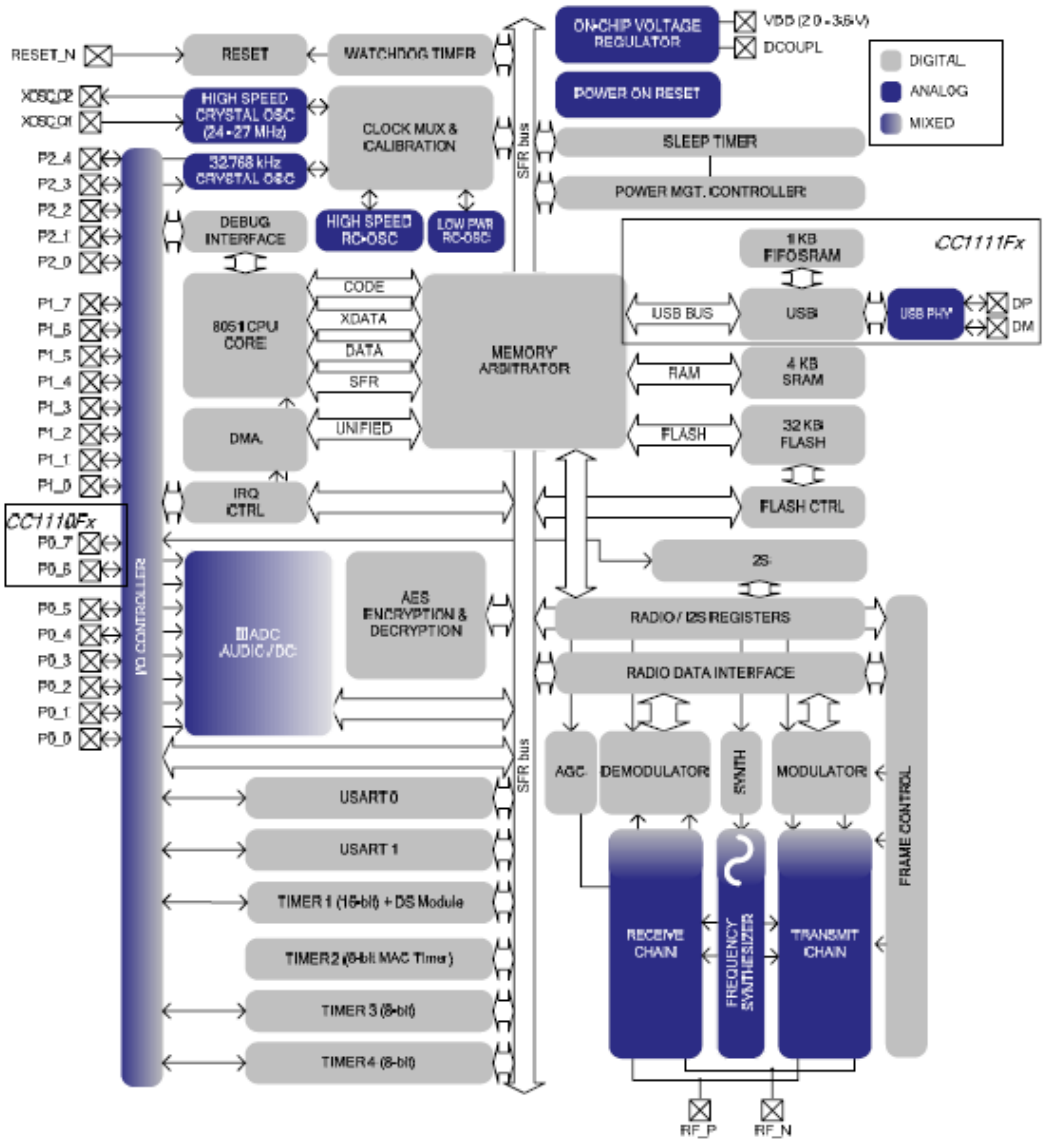

Figure 14: Block diagram of CC1110

- High-performance RF transceiver.
- Good selectivity and blocking performance.
- High selectivity (e.g. -110 dBm at 1.2 kBaud).
- Programmable data rate up to 500 kBaud.
- Programmable output power up to 10 dBm for all the frequencies.
- Frequency range: 300 – 348 MHz, 391 – 464 MHz and 782 – 928 MHz.
- Digital RSSI[3] support.
- Low power consumption.
- 8051 microcontroller core.
- DMA functionality.

[3] Received Signal Strength Indication, it is a measurement of the power present in a received radio signal.

- Up to 32 kB in-system programmable flash memory and up to 4 kB RAM.
- USB 2.0 interface.
- One 16-bit timer and three 8-bit timers.
- Two USARTs.
- 21 General Purpose Input/Output pins.
- 7 – 12 bit ADC with up to eight inputs.
- Hardware debug support.

Among all these characteristics, those which are key in the algorithm proposed later are: the RF functionality for making possible, obviously, the communication between base station and mobile terminal; the 433 MHz frequency band because is the band where the mobile terminal operates; the RSSI support since in the algorithm it will necessary to control the power received for different operating frequencies; the timers for scheduling the frequency sweep and for the synchronization.

Undoubtedly, the RF module of CC1110 is essential in the system design because it provides almost automatic control over various aspects related to the radio signal, such as channel and power configuration, modulation, data rate, packet handling and many other functions that this project may not require. A block diagram of the Radio Module is attached in *Figure 15*.

It should be noticed that the receiver part is a low Intermediate Frequency (IF) receiver. The received RF signal is amplified by the low noise amplifier (LNA) and down-converted in quadrature (I and Q components) to the IF. At this frequency, the I/Q components are digitized by the ADC blocks. From there, digital treatment of the signal (e.g. Automatic Gain Control (AGC), channel filtering, demodulation and packet handling) is performed.

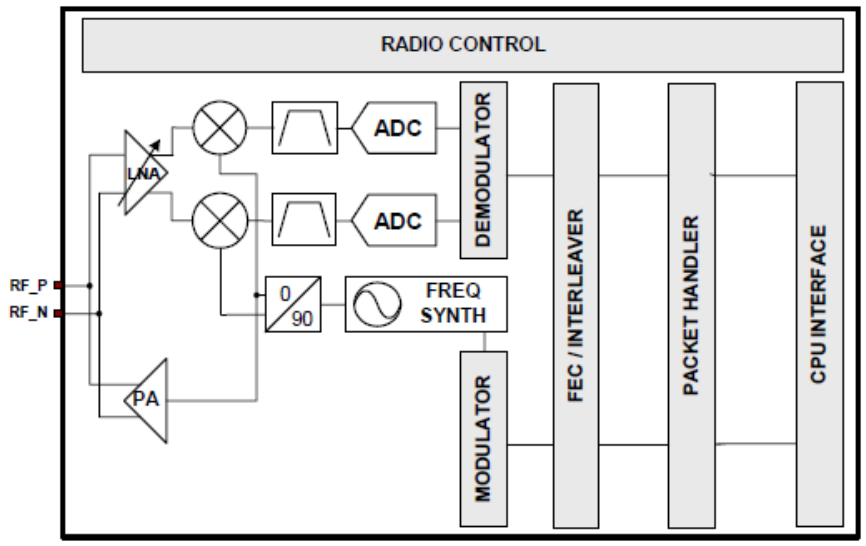

Figure 15: CC1110 RF block diagram

The transmitter part of the chip is based on direct synthesis of the RF frequency. The frequency synthesizer includes: a LC Voltage-Controlled Oscillator (VCO) and a 90 degrees

phase shifter, which is responsible for the generation of the I and Q signals to the down-conversion mixers in receive mode. The reference frequency for the synthesizer is provided by a 26/48 MHz crystal oscillator. This oscillator also generates clocks for all the digital modules.

Before starting writing the code for the algorithm, the datasheet of CC1110 provided by Texas Instruments was studied deeply in order to know how to manage all the registers. In the code, which is attached in the *Appendix C: Program codes* and written in C language, it is indicated the utility of the registers that controls different functions like timers o radio. Moreover, previously to write the code, it was necessary the development of little programs to get familiar with each part as well as test them separately. Later in this document, more practical issues about the algorithm and its codification will be discussed.

A Texas Instruments application, SmartRF Studio 7, was used for the radio registers configuration and test purposes. This facility allows programmers to set registers in an easy way and send/receive signals in all the formats that the CC1110 provides. For more details consult the *Appendix B: SmartRF Studio 7*.

3. Designing stage: antenna and algorithm

3.1. Design and fabrication of the base station antenna

3.1.1. Simulation

As it was said in *2.1*, the antenna for the mobile terminal was already designed and constructed while, in the case of the base station, only the CC1110 chip (with the corresponding port for the antenna) was available. Hence, the design, which includes computer simulations, and the construction of a new antenna was carried out.

There were two main requirements for this antenna: on one hand, the antenna had to cover the 391-431 MHz frequency bandwidth as it was explained in *2.1;* on the other hand, it was required a simple and easy-to-manufacture design. By contrast, size and portability limitations were not considered, so that the antenna did not have to be internal. In the following lines, the whole process is going to be described, that is to say, theoretical approach, simulation, construction and verification.

One of the simplest antennas known is the dipole antenna, so the first idea was to design a λ/2 dipole, discarding other options like loop or internal printed antennas. This kind of antenna provides an omnidirectional pattern, which makes it very suitable for a base station. As it was thought to mount the antenna vertically on the CC1110 the polarization of the radiated waves would be also vertical.

The dipole had to resonate at 410 MHz, which is approximately the center frequency of the desired bandwidth. However, since around 400 MHz a dipole would have been too long (in the order of 37 cm) and a differential feed (which is complicated to implement) is needed, a $\lambda/4$ whip antenna was chosen instead as a base station antenna. It is noticeable that the wires available in the laboratory to make the whip antenna consisted of a 1 mm diameter copper wire, so the diameter, which could help to improve the bandwidth, was not modifiable.

To create a monopole, an ideally infinite ground plane is needed which, by the effect of mirroring, will cause a dipole radiation pattern. In most cases, this ground plane is achieved by using the case of the mobile terminal if its dimensions are similar to the whip antenna. In the present project, thought, the whip had to be mounted on the CC1110, whose dimensions (29 x 33 mm) were not enough to make the ground plane. The chosen alternative was to simulate the ground plane by connecting four wires to the chip ground just in the base of the whip. The length of these wires was approximately the length of the whip, thus making a set of $\lambda/4$ open-ended stubs. They were placed equispacedly forming a kind of star. In *Figure 16*, the star structure of the ground plane can be observed, apart from the whole model, which is going to be commented.

After having the first model in mind, this was translated to a computer model and, afterwards, simulated. The software used was Ansoft HFSS[4] Version 11.0. It was included also the PCB structure with the ground and the substrate, which is made of FR-4. It was supposed that both antenna element and ground were perfect conductors, which is a good approximation for copper. First of all, the model was drawn using the tools provided by HFSS. The length of the $\lambda/4$ whip was calculated before as seen below. In *Figure 16* and *Figure 17* the complete graphical model is shown.

$$\lambda = \frac{c}{f} = \frac{3 \cdot 10^8 \frac{\mathrm{m}}{\mathrm{s}}}{410 \cdot 10^6 \ \mathrm{Hz}} = 731.7\mathrm{mm} \Rightarrow \frac{\lambda}{4} = 182.9 \ \mathrm{mm} \ \approx 183 \ \mathrm{mm}$$

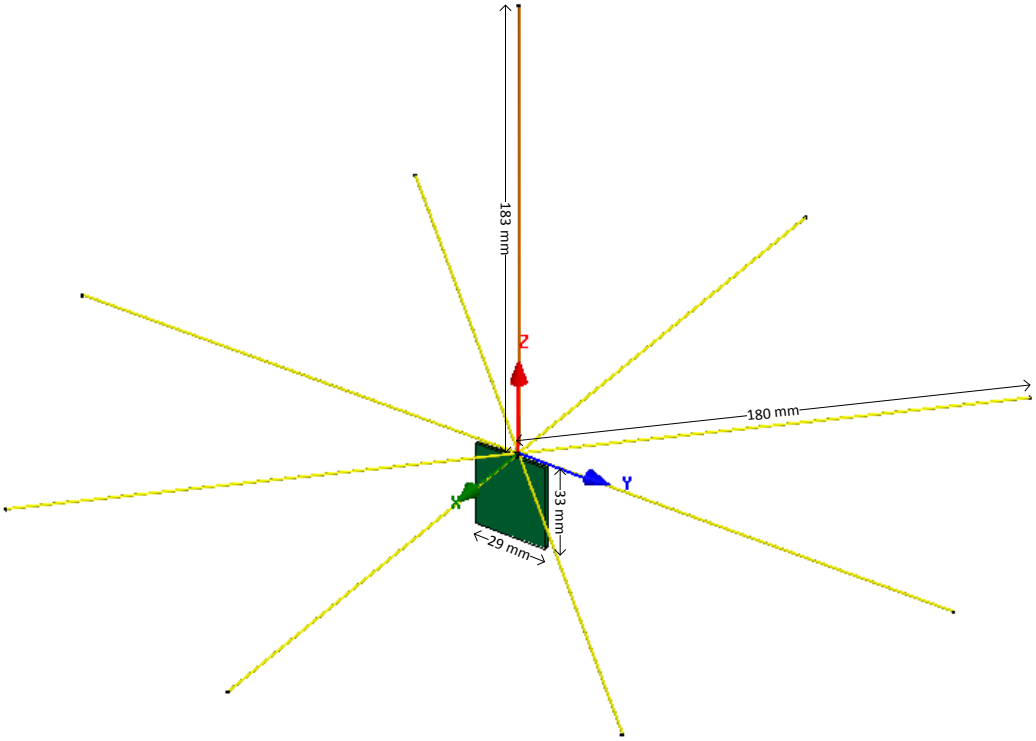

Figure 16: Complete view of the model base station antenna with dimensions (first version)

Once the model was finished and the excitations (50 Ω Lumped Port) and the radiation boundary conditions (far field conditions) were specified, the simulation settings were configured. It was selected a frequency sweep from 370 MHz to 450 MHz for the simulation because it was expected that the modeled antenna worked within this bandwidth. When the analysis was done, the following antenna parameters were obtained at 410 MHz:

- $Z_A = 21.50 + j14.96 \ \Omega$
- $S_{11} = -7.12 \ \mathrm{dB} \angle 140°$
- $\eta_{rad} = 1$ Because the radiating elements were supposed lossless.
- $G = D = 1.65$

[4] Ansoft HFSS is a FEM solver for electromagnetic structures.

- 3D Radiation pattern (see *Figure 18*). It can be observed that the radiation pattern is nearly omnidirectional, as was desired.

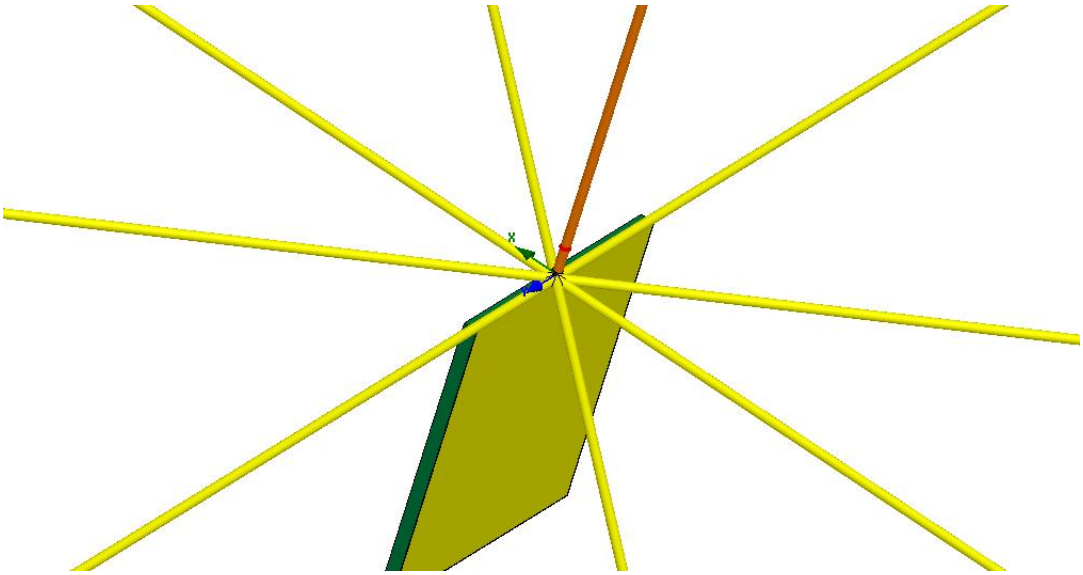

Figure 17: Closer back view of the designed antenna

From the parameters obtained above (e.g. input impedance quite different from 50 Ω), it was concluded that the antenna was not very well matched at the center frequency. This is also could be noticed in the plot of the S_{11} module over the frequency and its representation, module and phase, in the Smith Chart (see *Figure 19* and *Figure 20).* Even though in the frequency limits (391 and 431 MHz), the matching was not bad because the S_{11} is approximately -6 dB, within the whole bandwidth the matching was not good enough (as much it was achieved -7.2 dB at around 405 MHz), so a matching network was needed.

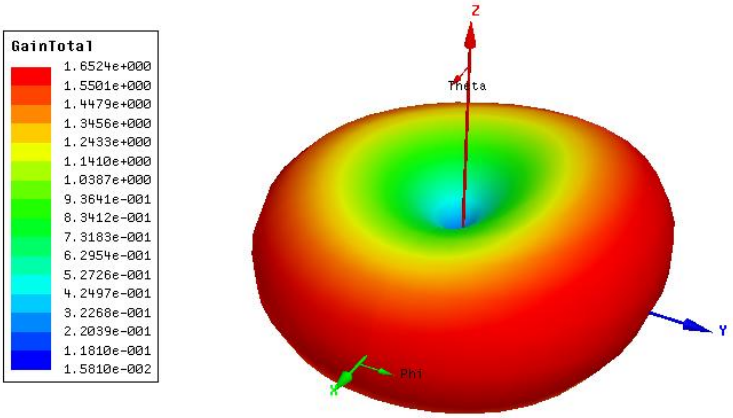

Figure 18: Radiation Pattern of the designed antenna

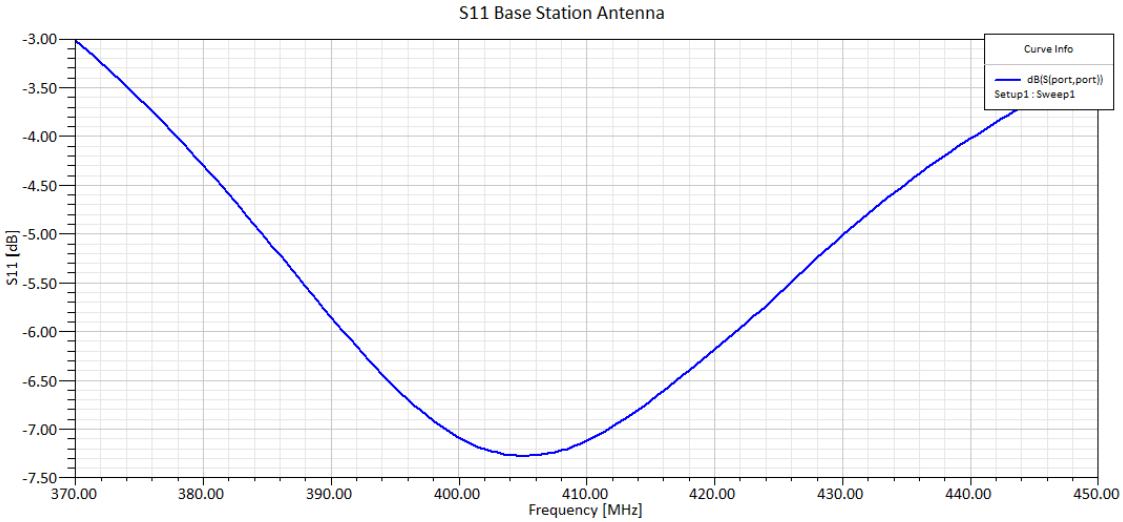

Figure 19: Module of the simulated reflection coefficient of the designed antenna (first version)

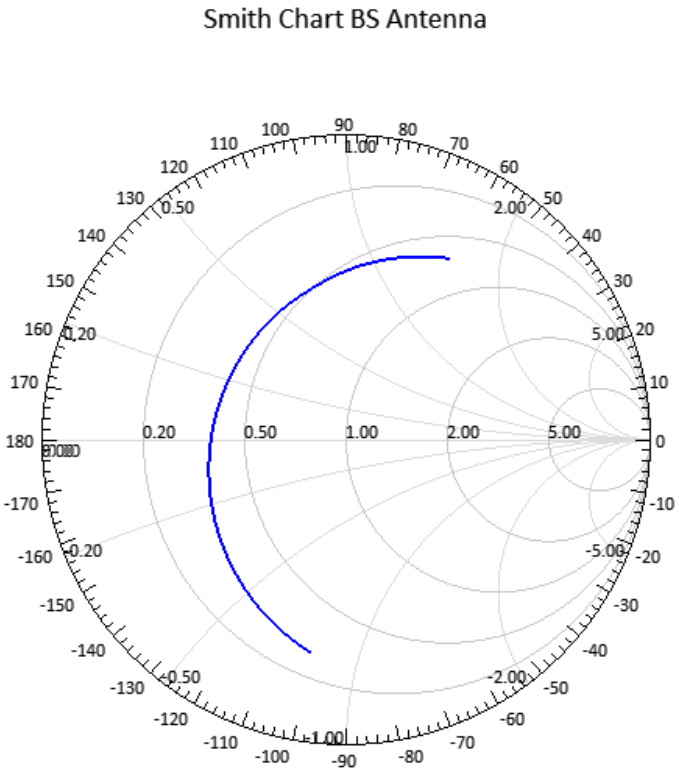

Figure 20: Smith Chart of the designed antenna (first version)

Since a simple matching network was required and the bandwidth which had to be covered was not too large (40 MHz, so larger than the mobile terminal bandwidth, though), a single matching element was considered sufficient. In addition, the fact that the length of the antenna could be modified made easier to obtain a good matching. The next step was to decide whether matching the antenna with a series or with a shunt element. The series element was discarded because is more difficult to solder it between the antenna node of the chip and the antenna itself, so a shunt matching was chosen. The element needed to be lossless (i.e. capacitance or inductor) in order to keep a high

antenna efficiency. Furthermore, it was decided to implement the matching element as a lumped element rather than a transmission line because the operating frequency was far away from the high microwave bands. A hybrid method, consisting of computer simulations with HFSS and manual calculations using basic circuit theory, was carried out to obtain the value of the matching element.

First of all, trough computer simulations, the length of the whip (maintaining the 180 mm length of the ground wires) that provided a real part of the input antenna admittance equals to the inverse of the generator impedance was searched. That is to say,

$$Re\{Y_A\} = \frac{1}{Z_g} = \frac{1}{50\ \Omega} \approx 0.02\ \Omega^{-1}$$

Once this is achieved and the length of the whip fixed, the imaginary part obtained with the simulation of the admittance had to be cancelled by the shunt element. It was founded two solutions: one of them required less length than the initially calculated and the other while the other required more length. On the other hand, depending on the solution selected, the shunt element was an inductor or a capacitor, respectively. Let's see how both solutions were calculated and the results of the HFSS simulations for each one.

Length was started to be decreased in steps of 1 mm from the initial value, which was 183 mm. A parametric simulation was carried out in HFSS for each value. At 169 mm the real part of the admittance was the desired:

$$Y_A(f = 410\ \text{MHz}, l = 169\ \text{mm}) = 0.0197 + j0.0289\ \Omega$$

Now the imaginary part of the admittance has to be cancelled taking into account that the input admittance of a shunt inductor and a shunt capacitor is the following:

$$Y_L = \frac{-j}{2\pi f L} \qquad Y_C = j2\pi f C$$

It was concluded that the necessary element was an inductor. Since the equivalent admittance of the shunt element and the antenna is equal to the addition of the admittance of each one, the value of the inductor (L) resulted:

$$j0.0289 - \frac{j}{2\pi f L} = 0 \Rightarrow L = \frac{1}{2\pi \cdot 410 \cdot 10^6 \cdot 0.0289} \approx 13.4\ \text{nH}$$

Figure 21 shows the equivalent circuit including the shunt inductor calculated above.

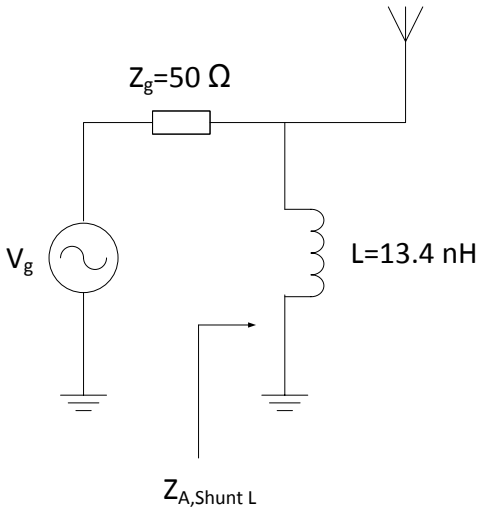

Figure 21: Equivalent matched circuit with shunt inductor

Next, the new value of the whip length was introduced as well as it was added a shunt lumped inductor whose value was 13.4 nH in the HFSS model. The simulation was restarted, and the antenna parameters for the shunt inductor matching were obtained at 410 MHz:

- $Z_{A,Shunt\ L} = 49.67 - j0.42\ \Omega$
- $S_{11,Shunt\ L} = -45.4\ \text{dB}\ \angle 127°$
- $\eta = 1$
- $G = D = 1.65$
- Omnidirectional radiation pattern.

Afterwards, the opposite operation was carried out. Length started to be increased in HFSS until the optimum value was found, which was 186mm.

$$Y_A(f = 410\ \text{MHz}, l = 186\ \text{mm}) = 0.0208 - j0.0216\ \Omega$$

In this case, the appropriate element that cancels the reactive part was a shunt capacitor. Its value was calculated in the same way as before:

$$-j0.0216 + j2\pi fC = 0 \Rightarrow C = \frac{0.0216}{2\pi \cdot 410 \cdot 10^6} \approx 8\ \text{pF}$$

The equivalent circuit (see *Figure 22*) is the same than the previous but replacing the inductor by the capacitor. Furthermore, the new parameters obtained from the HFSS simulation for the shunt capacitor matching at 410 MHz were the following:

- $Z_{A,Shunt\ C} = 50.30 - j\ 4.30\Omega$
- $S_{11,Shunt\ C} = -27.3\ \text{dB} \angle -83.5°$
- $\eta = 1$
- $G = D = 1.65$
- Omnidirectional radiation pattern.

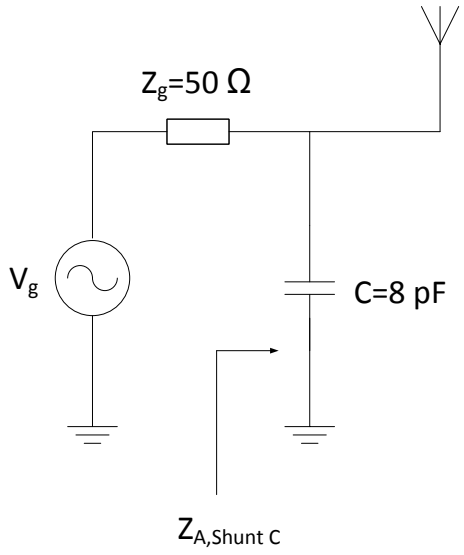

Figure 22: **Equivalent matched circuit with shunt capacitor**

When both solutions were simulated, a decision had to be taken. The criterion was to select the solution which provided higher impedance bandwidth. For this purpose, the reflection coefficient plots of each one were compared (*Figure 23* shows them). In the S_{11} plot corresponding to the shunt inductor solution, one can notice that at the central frequency (410 MHz), the minimum peak is more abrupt than in the case of the shunt capacitor. As a consequence, the impedance bandwidth is a bit larger for the capacitor solution. In the following table (*Table 1*), some numerical values related to the plots are shown.

Frequency (MHz)	Shunt inductor solution S_{11} (dB)	Shunt capacitor solution S_{11} (dB)
391	-4	-5.9
399	-7.7	-10.3
410	-45.4	-27.3
421	-8.7	-10.2
431	-4.7	-5.4

Table 1: **Numerical comparison between shunt inductor and shunt capacitor solutions**

It is observed that, if the whole frequency points are considered, the matching based on a shunt capacitor of 8 pF is better because it provides larger impedance bandwidth, so less power is lost because of reflection in most of the band (i.e. 391-431 MHz). The both impedance bandwidths at -6 dB of S_{11} are:

$$BW_{Shunt\ L} = 427\ \text{MHz} - 396\ \text{MHz} = 31\ \text{MHz} \rightarrow BW_{Shunt\ L}(\%) = \frac{31\ \text{MHz}}{410\ \text{MHz}} = 7.6\ \%$$

$$BW_{Shunt\ C} = 429.5\ \text{MHz} - 391.5\ \text{MHz} = 38\ \text{MHz} \rightarrow BW_{Shunt\ C}(\%) = \frac{38\ \text{MHz}}{409\ \text{MHz}} = 9.3\ \%$$

Therefore, the shunt capacitor was chosen as a matching element for the base station antenna, even though the whip would have to be longer.

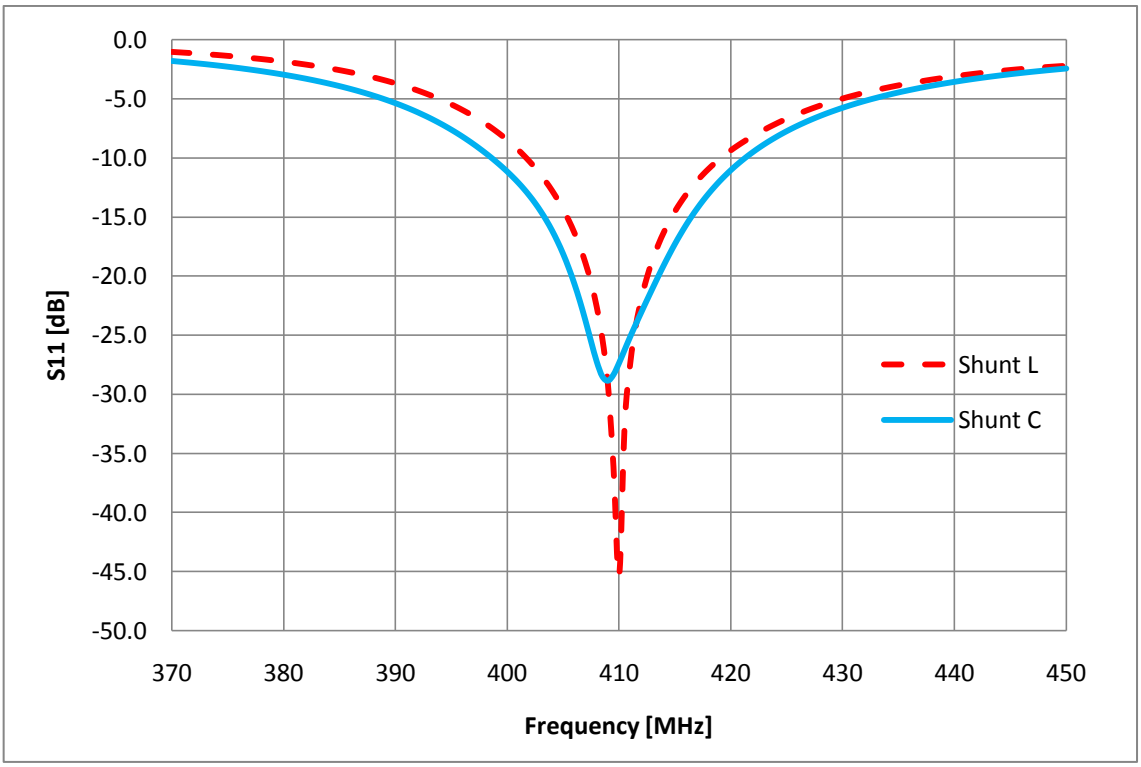

Figure 23: Simulated reflection coefficient of shunt inductor (red) solution and shunt capacitor solution (blue)

It is interesting to look at *Figure 24*, which shows the simulation of realized gain over frequency of the antenna matched with the shunt capacitor. It can be observed that for the frequency limits the gain loss with respect to the maximum gain is not too high (1.6 dB), which involves that this antenna is suitable for the purpose of the project.

To sum up and before describing the manufacturing stage, the antenna of the base station to be constructed has the next preliminary features:

- Whip antenna with a ground plane simulated by four crossed wires.
- The antenna is mounted on a chip whose dimensions are 29 x 33 mm.
- Whip length equals to 186 mm and ground plane wires length equals to 180 mm.
- Copper wires of 1 mm diameter.
- 8 pF shunt capacitor as a matching element.

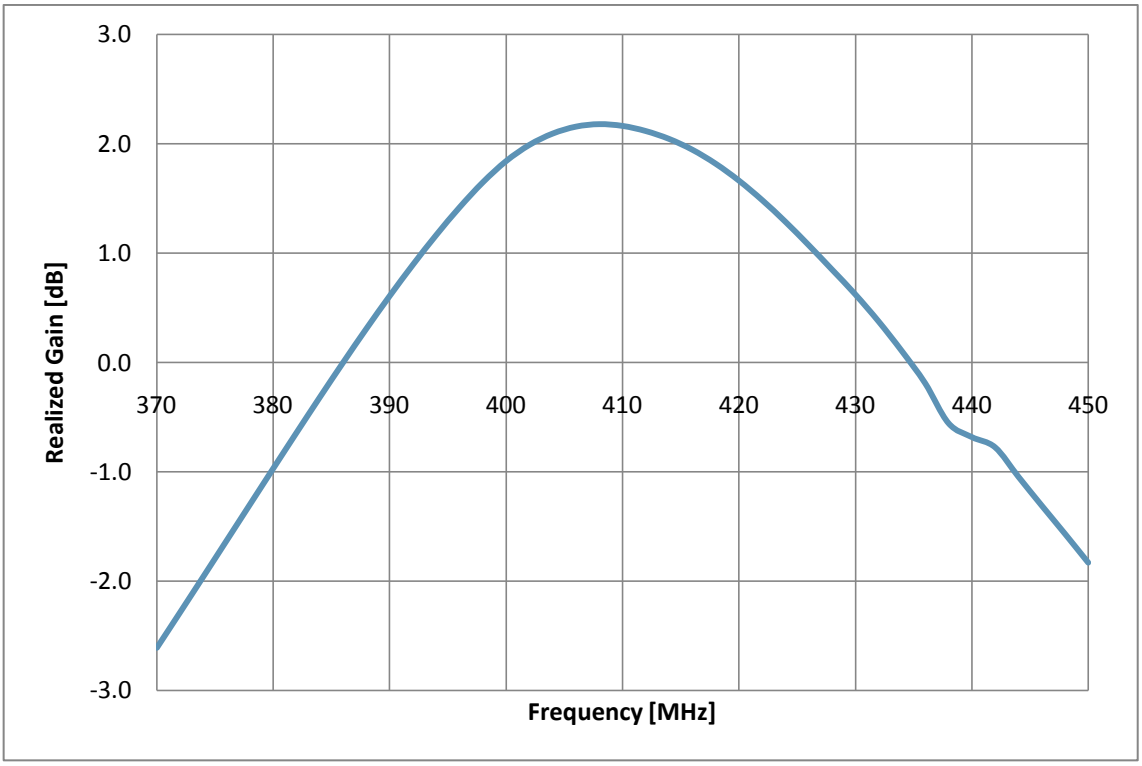

Figure 24: **Realized gain over the frequency for the shunt capacitor solution**

3.1.2. Fabrication and verification

In this section the followed steps to construct the simulated antenna for the base station are going to be detailed. First of all, an 8 pF capacitor was found and soldered onto the chip. One of its terminals was soldered to the ground of the chip, while the other one was soldered to the antenna terminal, which is placed on the top of the base station chip.

Later, enough quantity of 1 mm diameter copper wire was taken in order to make the different parts. Four wires, corresponding to the ground plane, of 180 mm length were cut, filed and arranged forming a star (see *Figure 16*). Immediately afterwards, the four wires were soldered with tin on the chip, thus connecting them to the ground of the chip.

The next step was to cut the whip wire slightly longer than the length predicted in the simulation. The reason for that was to ensure that the center frequency was approximately located around 410 MHz by making slowly shorter the whip while S_{11} plot was constantly visualized with the Vector Analyzer (to which the antenna was connected). Otherwise, if it had been cut the length found in the simulations (186 mm), it would have no chance to correct the possible discordance between the simulations and the real measurements. After cutting the wire (200 mm approximately), the whip was soldered to the antenna port of the chip perpendicularly to the ground plane, in the manner that had been modeled in HFFS.

Once all the components were put together, it was time to find the optimum length of the whip and see if it resulted similar to the simulated length. For this purpose, the device was tested using the Agilent N5247A Vector Analyzer, in the same way as the

mobile terminal antenna earlier. Starting from 200 mm, the whip was being cut until the length was 188 mm, where the minimum of the S_{11} was located around 410 MHz (408 MHz to be exact). Since the precision using this method was not too high, it was preferred not to continue cutting. The final aspect of the fabricated antenna is shown in *Figure 25*.

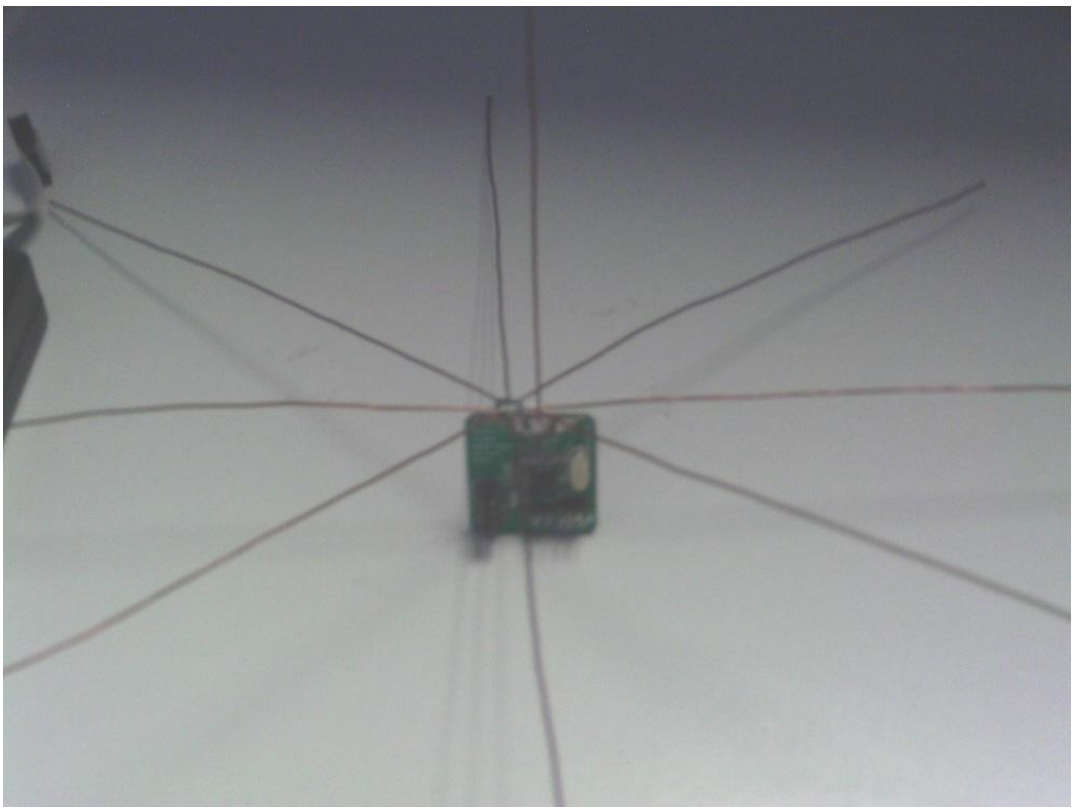

Figure 25: Fabricated base station antenna

The snapshot of the measurement of the S_{11} with the Agilent N5247A Vector Analyzer can be observed in *Figure 26*. At first sight, reading the information provided by the markers it was noticed that in the limits the value of the reflection coefficient was better. For more precision, see *Figure 27*, which shows the plot of the simulation of the reflection coefficient and the plot of the measurement of the same coefficient. It can be noticed that simulation and real measurement of the reflection coefficient agree quite well, but the second one contains more abrupt minimum peak. Even though it could have been possible to adjust even more the center frequency, that result was approved because almost the entire frequency points had less than -6 dB of S_{11} module.

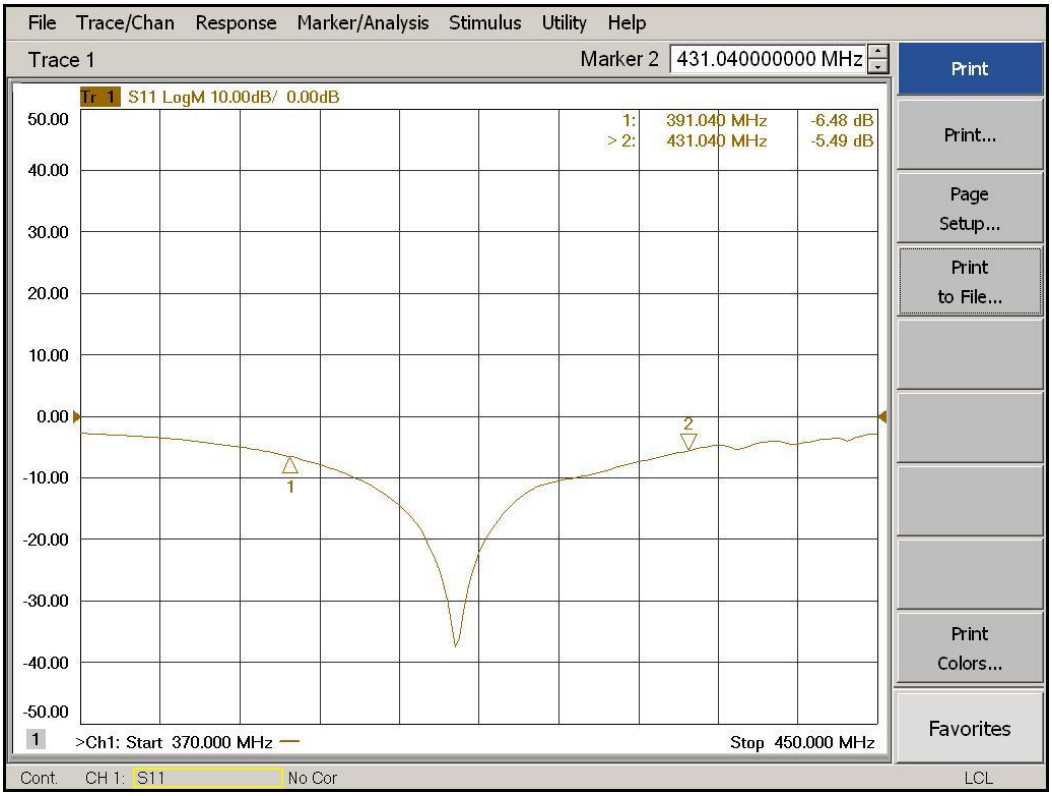

Figure 26: **Snapshot of the S_{11} measurement of the base station antenna**

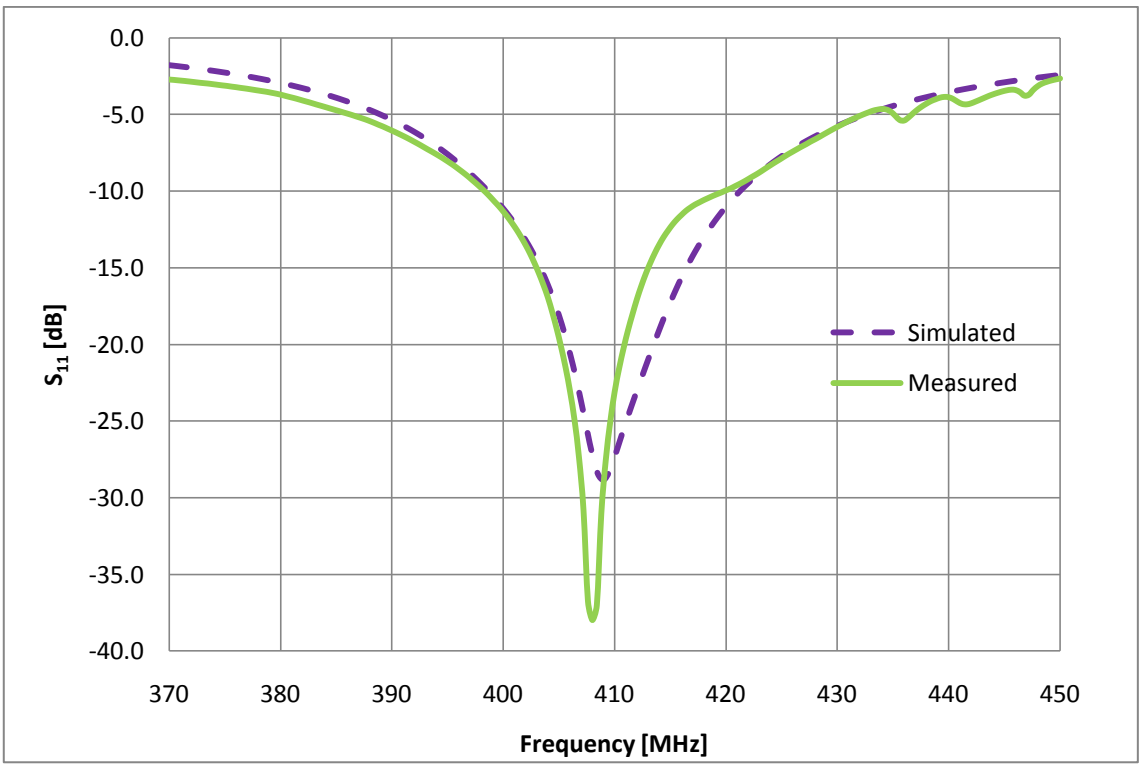

Figure 27: **Simulated (purple) versus measured (green) reflection coefficient of the base station antenna**

Below the bandwidth of the constructed antenna is calculated:

$$BW_{meas} = 429.6\ \text{MHz} - 390\ \text{MHz} = 39.6\ \text{MHz} \rightarrow BW_{meas}(\%) = \frac{39.6\ \text{MHz}}{408\ \text{MHz}} = 9.7\ \%$$

This result involves that the impedance bandwidth of the constructed antenna (9.7 %) is even better than the simulated (9.3 %).

After having finished the antenna for the base station, it was tested its performance using the application SmartRF Studio 7. Both base station and mobile terminal were connected to a computer trough USB port and the application was initialized. Each one was configured as a transmitter and receiver and it was verified that power was detected at some random operating frequencies. At the frequencies in which the reflection losses of the base station antenna were minimum, the power detected was around -21 dBm when transmitting 10 dBm and the separation between the two devices was 0.94 m approximately. This power level was considered a good result because the following reasoning. One can calculate the path loss between two antennas using the next formula:

$$L(\text{dB}) = 20\log\left(\frac{4\pi \cdot 1\ \text{m}}{\lambda}\right) + 10 \cdot n \cdot \log\left(\frac{d}{1\ \text{m}}\right)$$

Taking frequency 410 MHz (λ = 0.73 m), free space (n = 2) and distance 0.94 m (d = 0.94 m), the theoretical attenuation would be:

$$L(\text{dB}) = 24.2\ \text{dB}$$

The transmission equation, considering 2.2 dB of gain for base station antenna and -10 dB for the mobile terminal antenna (not real values, but extracted from the simulations), is:

$$P_r(\text{dBm}) = P_t(\text{dBm}) + G_t(\text{dB}) + G_r(\text{dB}) - L(\text{dB})$$
$$= 10\ \text{dBm} + 2\ .2\ \text{dB} - 10\ \text{dB} - 24.2\ \text{dB} = -22\ \text{dBm}$$

where P_r is the received power, P_t is the transmitted power, G_t is the gain of the base station antenna, G_r is the gain of the mobile terminal antenna and L is the path loss.

Since the operating frequency (410 MHz) and the center frequency of the base station antenna are the same, G_t is the maximum realized gain. By contrast, G_r is not the maximum realized gain because the center frequency of mobile device antenna is 430 MHz, so at 410 MHz the realized gain is lower than at 430 MHz (see *Appendix A: Mobile terminal antenna parameters* to understand such specific value). It can be noticed that the theoretical and practical results agree really well, thus approving the gain values obtained from the simulations.

When the results were validated, the designing stage of the base station antenna was considered ended. In this section the simulation and the construction of the aforementioned antenna has been described. Now, all the necessary physical elements for establishing a communication protocol are ready. The only element that is missing is

the essential one, that is the software containing an algorithm which is able to avoid the human body effect on the antenna performance. The design and the implementation in both, base station and mobile terminal, devices are going to be explained in the next section.

3.2. Software design and implementation

3.2.1. General description of the algorithm

As it was seen in *2.1.2*, the mobile terminal antenna is a narrow-band antenna whose center frequency point is displaced (impedance mismatching) to lower frequencies when a human hand is close to it. The negative effect is evident: the reflection coefficient is moved, so (supposing that at the initial operating frequency the return losses are low) losses due to reflected power far from the center frequency become quite larger. At this point, two assumptions are made: 1) the base station S_{11} remains almost constant; 2) the losses due to the possibility of not working in the center frequency of the base station are negligible compared to the same losses of the mobile terminal (see the pictures of realized gain in *Figure 24* and *Appendix A*: *Mobile terminal antenna parameters* for each device).

If absorption losses are added to the total attenuation of the signal, it could reach 10 dB because of the proximity effect, thus deteriorating the link quality and causing even an interruption of the communication. For minimizing this effect, an algorithm based on a communication protocol was designed and implemented on both link ends.

Roughly, the objective of the algorithm is to find the best frequency channel to start the communication. This channel should coincide with that where the new S_{11}, corresponding to the antenna which is affected by the human body presence, is minimum. Hence, the impedance is matched by varying the operating frequency. *Figure 28* exhibits graphically the expected behavior of the algorithm.

The base station sweeps all the bandwidth (391-431 MHz) transmitting power while the mobile terminal takes samples of the power level received (RSSI) for each frequency channel, thus following the base station. When the mobile terminal detects the highest RSSI, it lets the base station know which the best channel is. Then, both devices stop sweeping and normal communication can be resumed. The precision of the frequency steps when sweeping, the total time to rematch the antenna and other timing and power level considerations will be discussed later.

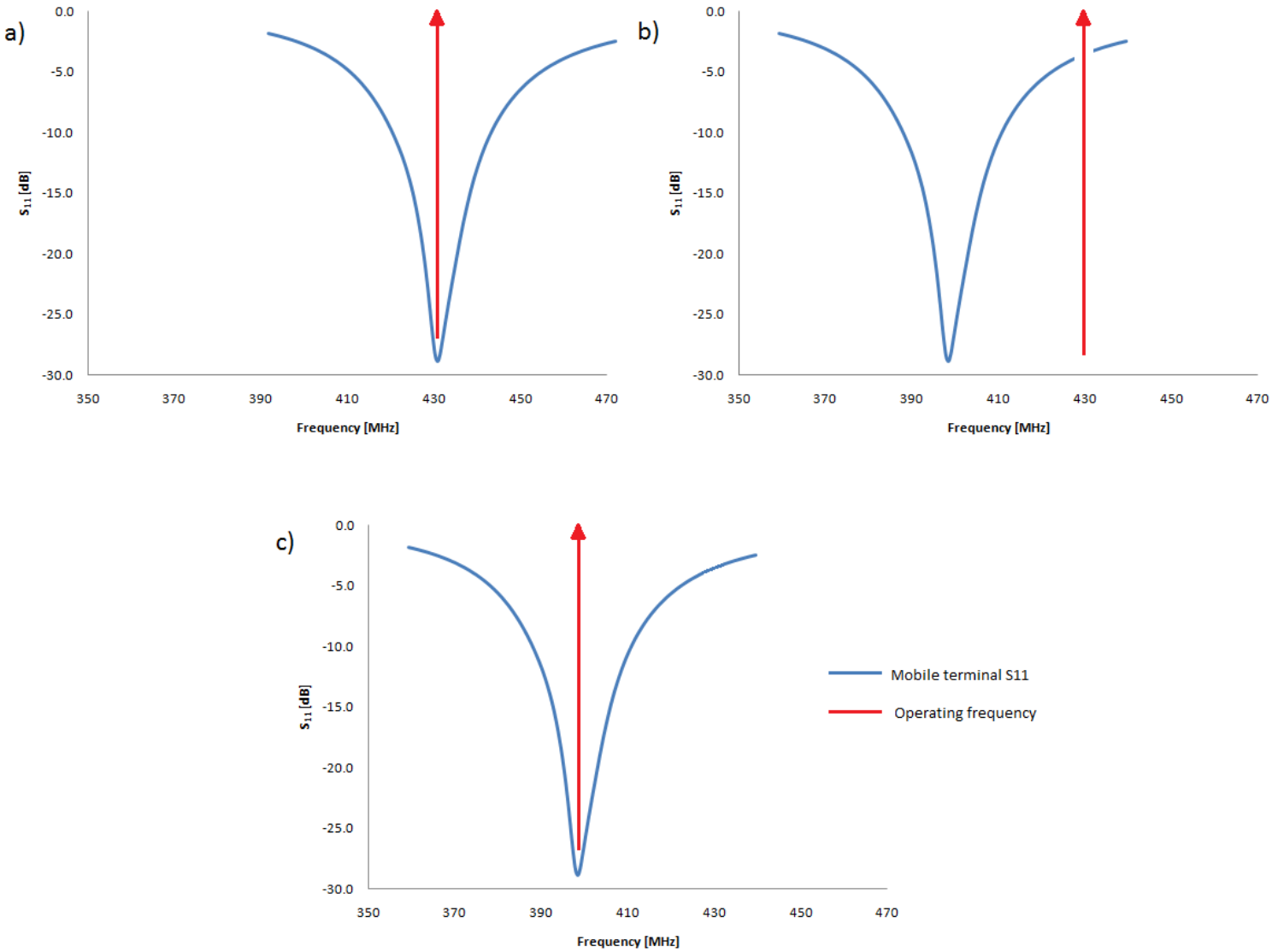

Figure 28: (a) Operation under perfect impedance matching conditions, (b) Mismatching effect due to human body presence, (c) Correction of the operating frequency to rematch the impedance

In the following lines the whole process until reaching the new matching condition is described. Firstly, though, a few useful abbreviations and variables, whose specific values are going to be discussed in following sections, are listed.

- BS: base station.
- MT: mobile terminal.
- *CH*: current channel being tested.
- CH_0: initial channel of the MT.
- CH_{BEST}: best channel found by the algorithm.
- *RSSI*: power present in *CH*.
- T_{SW}: frequency sweep period. It is the time between two consecutive variations of the signal operating frequency.
- T_{LIST}: listening time. It is the maximum time during the BS listen the channel to find a possible carrier which comes from the MT.

- T_{TX}: transmitting time. It is the time during the BS transmits the carrier that should detect the MT. The condition $T_{SW} = T_{LIST} + T_{TX}$ must be fulfilled.
- T_{COM}: communication time. It is the time during BS and MT transmit/receive carrier when the algorithm is in the final states.
- *BW*: system bandwidth. It is the frequency bandwidth which BS and MT have to sweep (391 - 431 MHz, justification in section *2.1*).
- CH_{STEP}: channel step. It is the frequency displacement from one frequency to the next when sweeping the *BW*.
- $N_{FC} = BW / CH_{STEP}$: frequency channels. It is the number of frequency channels that are tested.
- $T_{ALG} = 3 \cdot N_{FC} \cdot T_{SW}$: maximum algorithm time. It is the maximum time that the algorithm takes to find the new channel. This happens when the best channel is placed just before the initial channel of the MT.
- $RSSI_{TH}$: power threshold. It is the minimum power that is considered a valid signal. The power transmitted by one device and received by the other must be above this threshold.
- $RSSI_{BEST}$: best power level found among all the channels and corresponding to CH_{BEST}.
- Δ: sensitivity. Maximum power level difference (dB) between the best power received ($RSSI_{BEST}$) and the current power detected (*RSSI*) when the algorithm is in the final states.

When the MT is activated, starts to listen CH_0 inside the BW. Later, when the BS begins to run, sends a signal whose frequency corresponds to the first of the BW (i.e. 391 MHz). After T_{SW}, the BS stops transmitting and starts to listen the channel during T_{LIST}. If no carrier from MT is detected, the BS continues transmitting carrier during T_{TX} until the frequency has to be moved one CH_{STEP}. Then, begins to listen again, so the BW is swept by the BS following the sequence: …LISTEN -> TRANSMIT -> NEXT CHANNEL -> LISTEN… If the sweeping arrives to the last frequency (431 MHz), is restarted at the first one. Meanwhile, the MT stays listening the same channel until the BS reaches this channel. Then, if the MT detects a carrier, begins to sweep from its initial channel. The MT time has to change the frequency each T_{SW} in steps of CH_{STEP}. It must be assured that the parameters used in the BS and MT are the same in order to have them synchronized.

Once both devices are working at the same frequency, the MT has to test the *RSSI* for each channel in order to know what the CH_{BEST} (i.e. highest *RSSSI*) is. After the MT reaches its initial channel, continues sweeping until reaches the CH_{BEST} for second time. Then, the MT stops and starts to send a carrier whose frequency corresponds to the best channel found, while the BS makes another round (that is the reason of the factor 3 in the definition of T_{ALG}). When the BS station reaches the CH_{BEST} and detects a carrier that comes from the MT, sends an acknowledgment when the MT stops transmitting and begins to listen (the time that the MT had send signal was a bit longer than $N_{FC} \cdot T_{SW}$). Finally, the MT receives the acknowledgment from the BS and the communication starts in the CH_{BEST}. Each device transmits signal during T_{COM} while the other one receives it. If the communication is interrupted or the power received differs more than Δ from the

best power found (this may be caused by variations of the position of the body with respect to the MT), the algorithm is restarted to find a new CH_{BEST}, that is the BS starts to sweep and the MT stays listening.

To better comprehension of the algorithm that was implemented see *Figure 29* and *Figure 30*. One can observe the flowcharts concerning both devices. The variables used in the previous written description are reutilized for the state transition conditions. Notice that after ',' a modification of a variable comes, in this case, the change of the current channel.

In the next section the different values for the variables are going to be exposed as well as the considerations that were taken to choose that values. Afterwards, in the codification section (transform the flowchart into code), it will explained the working environment used to write the code, compile and debug, the descriptions of the relevant functions and so on. As a final point, in the verification section some tests, which were carried out when the code for the algorithm was written, will be shown. Those tests also helped to select the final values since various configurations were applied in order to find the optimum ones.

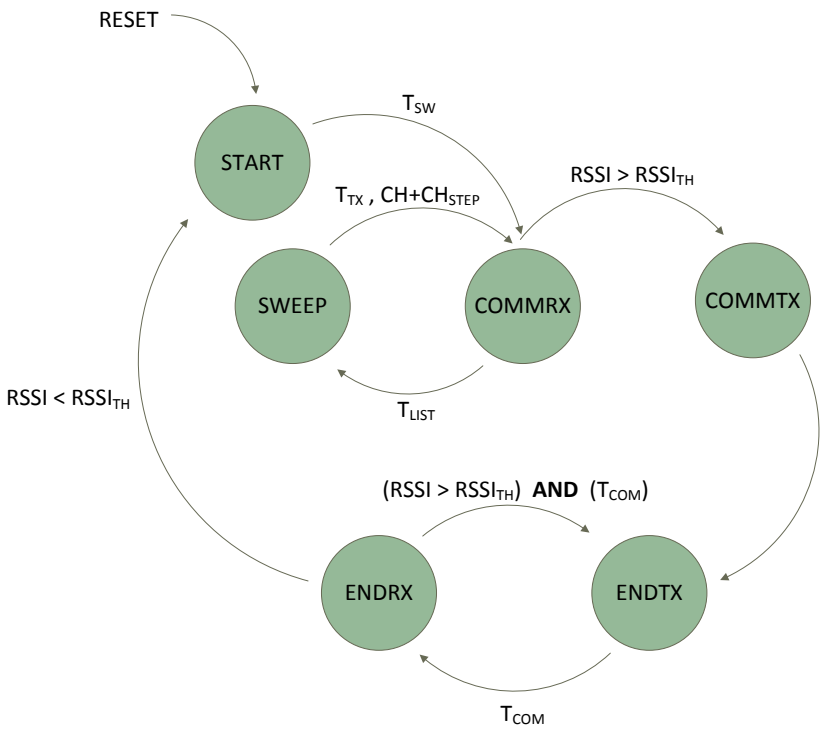

Figure 29: Flowchart of the algorithm implemented on the base station

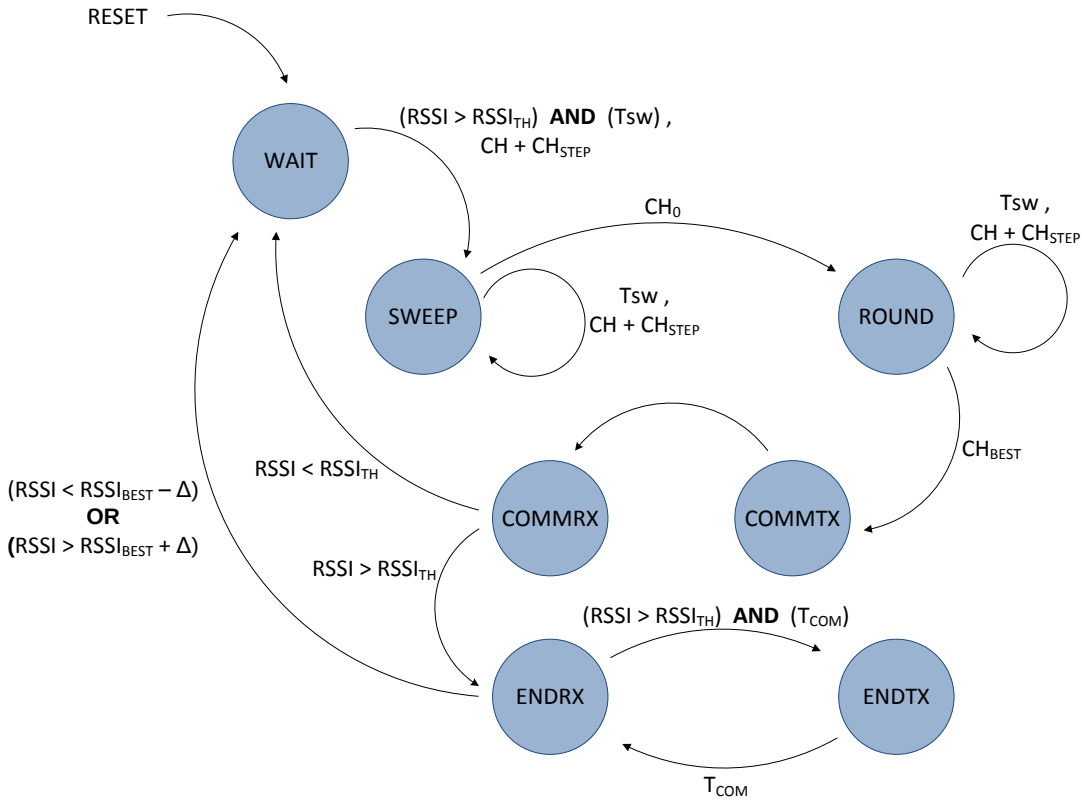

Figure 30: Flowchart of the algorithm implemented on the mobile terminal

3.2.2. Considerations and specifications for the algorithm

When designing the algorithm, the values for the variables introduced before were assigned. Some of them were thought during the designing process and some other during the test process in order to select the most appropriate number. Below, the values that were chosen are shown as well as the reasons contemplated to take such decision.

3.2.2.1. Timing

Basically, it was necessary to select the value of T_{SW}, because the other timing values are fixed by this one (except T_{COM}). T_{SW} is the parameter that determines, together with N_{FC}, the total duration of the algorithm, hence its importance. This time could not be extremely low since the chip CC1110 needs some internal time to do some operation, such as mode switching (e.g. transmitting to receiving mode), frequency recalibration or *RSSI* update. As a consequence, if a T_{SW} too short had been selected, the systems would not have enough time to perform all the programmed operations.

If the CC1110 datasheet is examined **[10]**, one can find the timing for key state transitions. It can be noticed that the maximum transition time is about 900 µs, so if the algorithm required four transitions per frequency jump, T_{SW} had to be 4 ms at least. Moreover, the update time of the *RSSI* depends on the configuration of the radio module, such as data rate, channel bandwidth, etc. Anyway, this update time is around 500 µs as much, so if we needed some RSSI samples (in the BS and MT), some more ms had to be added to T_{SW}. Therefore, a lowest bound for T_{SW} could be 10 ms.

Two other longer values were tested: 25 ms and 50 ms, apart from those used in early tests that were much longer. Even though choosing the lowest value of T_{SW} that provided a faster execution of the algorithm, the probability of de-synchronization between BS and MT may increase. However, multiple tests proved that even using the lowest time, the reliability of the algorithm was quite high. Another parameter that takes part in the reliability is T_{LIST} (and, hence, T_{TX}) since it determines if there is enough time to detect the incoming carrier and its peak power level. In order to make equals the listening times for both BS and MT, T_{LIST} was set to $0.5 \cdot T_{SW}$, so T_{TX} was also $0.5 \cdot T_{SW}$.

In *Table 2* the resulting values for the different time variables are specified.

T_{SW}	T_{LIST}	T_{TX}	T_{ALG}[5]
10 ms	5 ms	5 ms	600 ms
25 ms	12.5 ms	12.5 ms	1500 ms
50 ms	25 ms	25 ms	3000 ms

Table 2: Algorithm timing values

With regard to T_{COM}, it was set to 2000 ms and it controlled the time to restart the algorithm in case of an interruption of the communication or a change in the influence of a body on the MT antenna performance. It could have been set to a lower value if it had been desired.

3.2.2.2. Power

There were a few aspects that involved the concept of power. On the one hand, the transmitted power since CC1110 brings the opportunity to transmit signals with various power levels. In this project, the levels 10 dBm, 0 dBm and -10 dBm were tested in both links. Obviously, the higher power, the longer range, so the power level used depends on the application purpose. In addition, the fact that the system works in ISM/SRD bands should give preference to low levels of power with the aim of avoid interfering other devices, which are probably using the same band.

On the other hand, the power which is considered a valid signal coming from the other device ($RSSI_{TH}$) was a relevant parameter to be selected. From the application SmartRF Studio 7, it was known that the received power without a carrier present (so only receiving noise) was around -100 dBm, using a data rate of 5 kBaud. Therefore, it was chosen $RSSI_{TH}$ = -80 dBm, so that a possible interference could be only 20 dB above the noise floor. Increasing this value could produce a system failure since the carrier from the system devices would be considered as a valid system signal. Moreover, the distance between the BS and the MT as well as the distance between the whole system and other interfering devices could restrict the $RSSI_{TH}$.

[5] Taking N_{FC} = 20, the reason is given later.

Another parameter related to the power is *Δ* because is a measure of the sensitivity of the system versus antenna impedance changes, which are caused by body proximity with respect to the antenna. It was observed, with the help of SmartRF Studio 7, that at 410 MHz, the power loss in the MT device caused by the proximity of a bottle plenty of water (see chapter *4* for practical details of the experiments) was about 3 dB when the bottle was placed 1.5 cm away from the antenna. Hence, was considered that values between 3 and 5 dB were acceptable for *Δ*. A value below 3 dB could cause a non-necessary initialization of the algorithm because of objects which were placed further than the operator or whose presence was short in time. On the contrary, a high value of *Δ* could require a very hard effect of the body on the antenna that could not be achievable. However, it was considered that, in the limit case, a *RSSI* loss of 5 dB was enough to think that the antenna was under the influence (constructive or destructive, depending of the operating frequency) of a human body.

3.2.2.3. Channelization

The selection of how much larger should be the frequency jump when sweeping the bandwidth determines the number of channels to test. Consequently, as it was mentioned in the timing section, the channelization also affects directly to the total time of the algorithm.

Two aspects were contemplated when deciding CH_{STEP}. The first one was the antenna impedance bandwidth of the MT, which is 7.5 MHz (at -10 dB) approximately. As it was desired to have a certain level of accuracy, CH_{STEP} could not be greater than this value. The second factor taken into account was the coherence bandwidth (B_C) of the communication channel, which depends mainly on the environment where the system works and its propagation conditions. In **[11]** the experimentally measured values which correspond to the delay spread (D) for different scenarios are shown. In a bad case, such as the system working in the laboratory where was designed, the root mean square of the delay spread is 56 ns, so the coherence bandwidth:

$$B_C \approx \frac{0.1}{D_{rms}} = \frac{0.1}{56\ \text{ns}} = 1.786\ \text{MHz}$$

This value means that there is no significant variation of the communication channel over approximately 1.8 MHz. If it had been chosen a value much lower than 2 MHz, two values of *RSSI* at two consecutive random frequency channels would have a high probability of being the same, thus making the algorithm inefficient. Once these two aspects were analyzed, it was conclude that CH_{STEP} had to fulfill the next condition:

$$1.8\ \text{MHz} < CH_{STEP} < 7.5\ MHz$$

Finally, the value selected was 2 MHz, so the number of channels was:

$$N_{FC} = \frac{BW}{CH_{STEP}} = \frac{40\ \text{MHz}}{2\ \text{MHz}} = 20\ \text{channels}$$

3.2.2.4. Other parameters

There were some other variables that have not been mentioned before and did not take part directly in the algorithm performance. They were the signal modulation, the data rate, the deviation, the channel spacing and the receiver filter channel bandwidth. In the following lines there is a brief comment of each one:

- Modulation. CC1110 provides four kinds of modulation, which are 2-Frequency-Shift Keying (2-FSK), Gaussian FSK (GFSK), On-Off Keying (OOK) and Minimum-Shift Keying (MSK). It was selected GFSK, which is a type of FSK that uses a Gaussian filter over the modulated FSK signal to smooth it. FSK consists of a carrier whose frequency changes between two values, thus producing two different symbols (0 or 1). The demodulator notices the transmission of different symbols because of the frequency variation of the signal.
- Data rate. It can be chosen from 1.2 kBaud to 500 kBaud. It was observed that for 500 kBaud (so large receiver bandwidth was required) the noise floor was around -80 dBm and its variance was high. Consequently and since a high level of noise could cause that the system did not work correctly, the data rate was set to a lower value (5 kBaud).
- Deviation. It is the difference between the carrier frequencies of each symbol of the FSK signal. It was choosing taking into account the data rate and the bandwidth of the receiver, so that its value was 9.5 kHz.
- Channel spacing. It was the frequency separation between two CC1110 channels, which did not coincide with the system channels. However, the CH_{STEP} had to be a multiple of this parameter. The value selected was 200 kHz, so a jump in the algorithm was equivalent to 10 CC1110 channels displacement.
- Receiver filter channel bandwidth. It was set to 58 kHz (minimum allowed by CC1110) that was enough to filter the desired signal.

3.2.2.5. The need of data packets

CC1110 gives the opportunity of implementing transmission and reception of packets with a personalized format. Although the incorporation of packets could have made the system more robust, it was opted to use only carriers which contained random bits. This decision facilitated the programming of the code (implementing packets required to handle DMA function of CC1110) and reduced the algorithm execution time. In the final chapter, the benefits that could provide the communication trough packets between BS and MT will be analyzed.

3.2.3. Program code description

The code of the algorithm was written in C language and the development environment utilized was IAR Embedded Workbench which is development software that supports many manufacturers and chips. In this environment the code could be edited, compiled and afterwards debugged directly on the device, which was connected to the computer trough an USB port.

Once created a workspace (one for the base station and the other for the mobile terminal) in which the C files were included, it had to be specified the chip (CC1110) and the core (8051) corresponding to the board on which the program developed was going to be run. *Figure 31* presents a snapshot of IAR Embedded Workbench aspect in debug mode. It can be noticed that there is a windows called "Disassembly" where the values of the chip registers are shown. This combined with the breakpoints were useful to control the program flow and correct the problems encountered during the process. Furthermore, there is a watch where the value of the variables could be consulted.

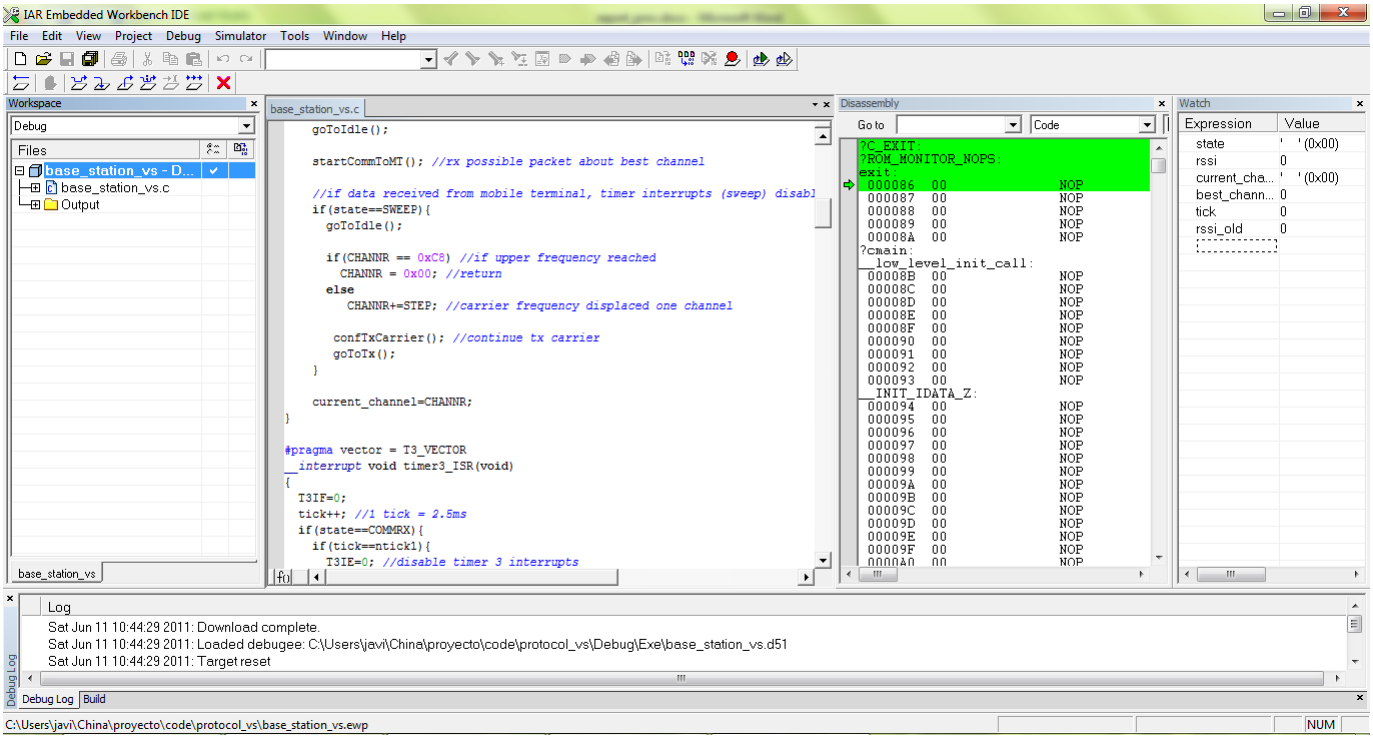

Figure 31: Aspect of IAR Embedded Workbench in debug mode

Before start writing the code for the base station and the mobile terminal, it was necessary to practice with small programs to get familiar with the different functions, such as LEDs, timer, radio and interruptions handling. To generate the correct configuration of the radio registers the aforementioned SmartRF Studio 7 was used.

When enough experience was achieved, the first stage was coding the frequency sweep part, which is related to the states START, WAIT and SWEEP of the flowcharts shown in *Figure 29* and *Figure 30*. A timer was used to control the frequency jumps of the base station every T_{SW}, while in the mobile terminal was programmed a carrier sense interrupt. That is to say the mobile was listening the initial channel until it sensed a carrier and then, if the detected power was above the threshold, an interrupt occurred and the mobile terminal began also to sweeping. It was programmed that the signal transmitted by the mobile terminal consisted of random bits, which were generated by the Random Number Generator of the CC1110. For each channel, the mobile terminal captured some samples of the power level detected and if any of them was above the last best sample of a previous frequency channel, it was stored in an array. As it was explained in the general

description of the algorithm, this sweeping stage finished when all the bandwidth was tested.

The next part to code was the communication process between the base station and the mobile terminal, which corresponds to the states COMMRX, COMMTX, ENDRX and ENDTX of the flowcharts. As it was mentioned before, no packets were used in the communication protocol, but only carriers containing random data. During this stage it was necessary to pay special attention to the times described in the timing section and program them carefully using the timers of the CC1110. Moreover, when one of two devices was in receiving mode, the threshold condition for the power was to be fulfilled to carry out the transition to the next state.

The whole code is shown later in *Appendix C: Program codes*, and now some functions corresponding to both programs are described briefly below. It has to be noticed that although most of the functions have common names, they may not contain the same code for both devices.

- **void initSettings().** Routine that initializes the LED's, the CC1110 clock, the RF module, the timers, the interruptions and a few variables.
- **void reset().** Reset all the variables and registers to their initial values. It is useful to return to the first state.
- **__interrupt void timer1_ISR().** Interruption routine related to the first timer. It controls the timing of the frequency sweeping.
- **__interrupt void timer3_ISR().** Interruption routine related to the third timer. It controls the times T_{TX} and T_{LIST}, thus the stopping of the sweeping state and the transition the COMMRX and COMMTX states.
- **__interrupt void timer4_ISR().** Interruption routine related to the forth timer. It controls the time T_{COM}, so the final states (ENDRX and ENDTX) when the devices are communicating trough the best channel.
- **__interrupt void radio_ISR().** Radio interruption routine configured only for carrier sense interruption. It is used to detect when the other device is transmitting.
- **int absRSSI().** Routine that obtains the power level detected in dBm.
- **void goToTx().** Transition to the radio transmitting mode.
- **void goToRx().**Transition to the radio receiving mode.
- **void confTxCarrier().**Configure the appropriate registers before going to the transmitting mode.
- **void confRxCarrier ().** Configure the appropriate registers before going to the receiving mode.
- **void goToIdle().** Transition to the idle mode, which is necessary to recalibrate the radio settings.
- **void testChannel().** Mobile terminal exclusive function that gets the power present in a channel and compares this value with the last one in order to determine whether is better or not.
- **void startCommToBS().** Mobile terminal exclusive function that begins communication with the base station when the best channel is found after

the sweeping stage. It covers the states COMMTX and COMMRX of the mobile terminal algorithm.

- **void startCommToMT().** Base station exclusive function that begins the communication with the mobile terminal if an incoming carrier is detected.

This has been a short description of the code that was developed. Obviously, the entire process was longer than it can be supposed by only reading the previous lines. In fact, the code was being tested and corrected gradually (e.g. verification of the frequency sweeping using a Spectrum Analyzer), thus making the process longer and more complex.

The next subsection is going to deal with a performance test done just after the code was finished (i.e. a final test apart from the partial tests aforementioned). The actual experiments under different conditions were carried out later and are going to be related in *Chapter 4*.

3.2.4. Algorithm performance first verification

When the code was finished, both devices, with its antennas, were connected each one to a PC trough an USB port (see *Figure 32*). Then, the programs were debugged and downloaded to its corresponding boards. Both programs were run and the following points were checked to determine if the algorithm worked as was expected.

Figure 32: Connection of the PCB to the computer trough USB

1. The mobile terminal remained in the wait state until a carrier appeared in its listening channel.
2. When the operating frequency of the base station in the sweeping state coincided with the listening frequency of the mobile terminal in the waiting state, the mobile terminal started also sweeping and the synchronization was not lost.
3. After some final adjustments, all the timing worked as expected. The times that were not specified in the timing section, were decided experimentally at

this stage. These times included the transmission times in the states COMMTX and COMMRX and the timeouts in the receiving modes.

4. The mobile terminal stopped when it was supposed and notified correctly to the base station of that.
5. Alternatively, both devices transmitted and received carrier in the final states.
6. During ENDRX and ENDTX, the algorithm was restarted if a bottle was situated near the mobile station antenna. Various values of the sensitivity Δ were tested and it was verified the lower the value was, the shorter the distance (between body and antenna) had to be to produce detuning.
7. The programs were stopped when they reached the states ENDRX/ENDTX and values of different variables were checked. For example, it was checked that both devices had the same operating frequency as well as the fact that the power levels stored by the mobile antenna followed an increasing tendency before reaching the highest RSSI.
8. The program restarting and the new execution were done correctly.
9. The system worked fine for the three times of execution that were planned: 600, 1500 and 3000 ms. These times were checked with an external clock.

4. Experiments and results

The next stage after finishing the code for the base station and mobile terminal was to test the algorithm that had been developed. Basically, some experiments were carried out to see if the algorithm was able to reach the main objective of the present project, which is to minimize the effect on the antenna performance when is affected by the proximity of a human body.

Since phantoms were not available in the lab to simulate the effect of a human hand or head and the use of real parts was not stable enough (i.e. difficulty when measuring the relative position with respect to the PCB antenna), another object had to be utilized instead. The object chosen was a cylindrical bottle plenty of water because it had similar relative permittivity (around 40 at 400 MHz) to the human muscles. The dimensions of the bottle were approximately 11 cm height and 7 cm diameter and, when simulating the human body effect, it was placed as shown in *Figure 33*.

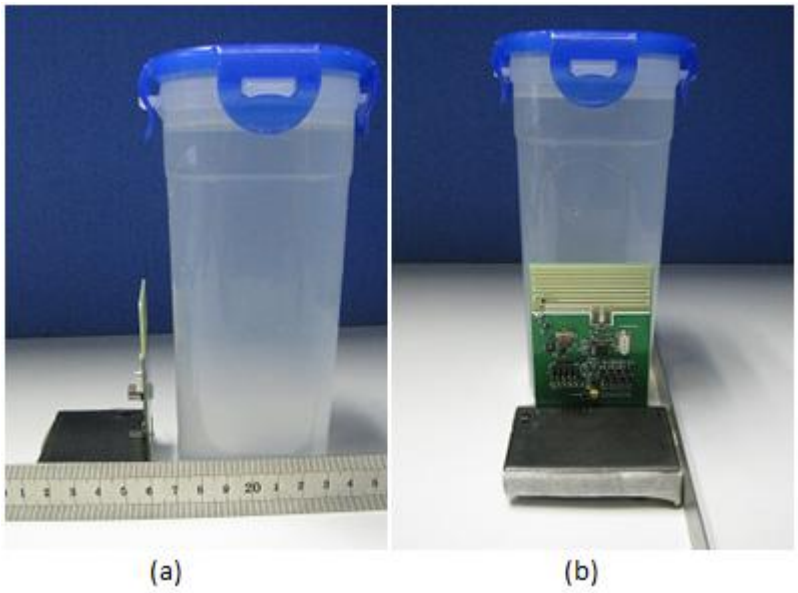

Figure 33: PCB and bottle positions: side (a) and frontal (b) views

The experiments were carried out in two environments: firstly, inside the laboratory and, secondly, in a garage, downstairs. The characteristics of each environment were quite different. While in the first case the devices were situated close to each other and under multipath conditions, in the second case the devices were placed further away and the effects of reflections were less important. The procedure was the same in both cases, and consisted of connecting each device to a laptop, running the program under different levels of bottle effect and taking notes of the results provided by the program variables. Furthermore, in the laboratory experiment, it was measured the improvement of the RSSI (dB units) that was achieved compared with the absence of algorithm, that is keeping the initial operating frequency.

4.1. Experiments inside the laboratory

The algorithm parameters used in this first set of experiments were the followings (go to *3.2.1* to remember some variable meanings if necessary):

- Total system bandwidth: 391 – 431 MHz
- Distance between base station and mobile terminal: 94 cm
- Transmitted power in both directions: 0 dBm
- T_{SW} = 25 ms
- CH_{STEP} = 2 MHz, so N_{FC} = 20 channels and T_{ALG} = 1500 ms
- Δ = 5 dB. This value did not matter because the program was restarted manually every time in order to record the measurements.
- Bottle placed behind the mobile terminal, so did not interfere in the direct path which comes from the base station.

As seen before, the best channel found when the algorithm is finished is denoted as CH_{BEST} (in MHz) and the level detected at this frequency is $RSSI_{BEST.}$ (in dBm) Furthermore, the power detected with the bottle present in the best channel that was found by the algorithm in absence of the bottle is denoted as $RSSI_{NA}$ (it was not an algorithm result, but it was measured using SmartRF Studio 7). This value allows calculating the improvement (i.e. $G_{SYS} = RSSI_{BEST} - RSSI_{NA}$) that provides the system with respect to that no frequency correction algorithm had been applied. This improvement is also the total power lost because of the proximity of a body. Another interesting indicator is the frequency difference (f_{DIFF}) between the best channel found with no bottle and the rest of situations. *Table 3* presents the results for different distances (D_{BOTTLE}) between the bottle and the PCB of the mobile device.

D_{BOTTLE}	CH_{BEST}	f_{DIFF}	$RSSI_{BEST}$	$RSSI_{NA}$	G_{SYS}
No bottle	419 MHz	-	-32 dBm	-32 dBm	-
1.5 cm	397 MHz	22 MHz	-37 dBm	-40 dBm	3 dB
1 cm	395 MHz	24 MHz	-36 dBm	-42 dBm	6 dB
0.5 cm	391 MHz	28 MHz	-39 dBm	-50 dBm	11 dB
0 cm	391 MHz	28 MHz	-40 dBm	-57 dBm	17 dB

Table 3: Results of the laboratory experiment

At first sight, the results agree with what was expected. It can be observed that the frequency of the best channel found decreases when the bottle is near the antenna (see *Figure 34* to appreciate it graphically). As it was analyzed in *2.1.2*, the results show that the center frequency of the mobile terminal antenna (minimum value in the S_{11} plot) is displaced to a lower frequency when there is body influence because the programmed algorithm moves the operating frequency of both devices to that new center frequency. In addition, it can be noticed that when the bottle gets closer to the antenna, the best

channels that the algorithm provides becomes lower. This is just what it was observed when measuring the S_{11} with the Vector Analyzer.

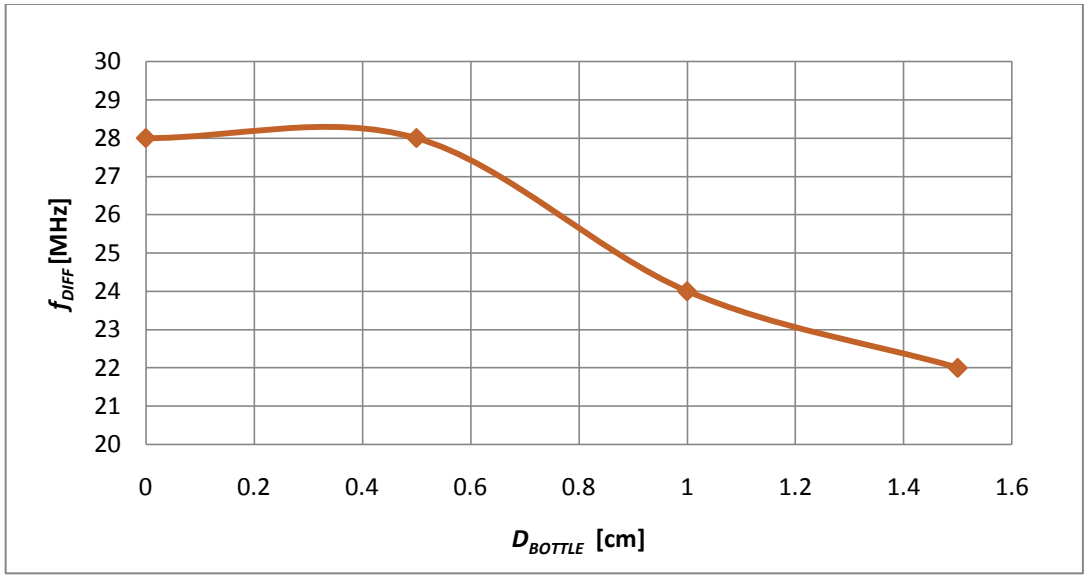

Figure 34: Frequency difference between the best channel found with no bottle and that one found with bottle at different relative distances

Apart from the frequency information, it was available to check the power received in the mobile terminal. It can be observed that the power in the best channel never is the same as when there is no bottle present. This is due to the fact that the water bottle absorbs a certain amount of power that comes from the base station even though the detuning effect has been correctly compensated. This power absorption degradation would have been more severe if the bottle had been placed between the base station and the mobile terminal and not behind the mobile terminal. This effect cannot be eliminated completely with the implemented algorithm, but the system was neither designed to deal with such effect.

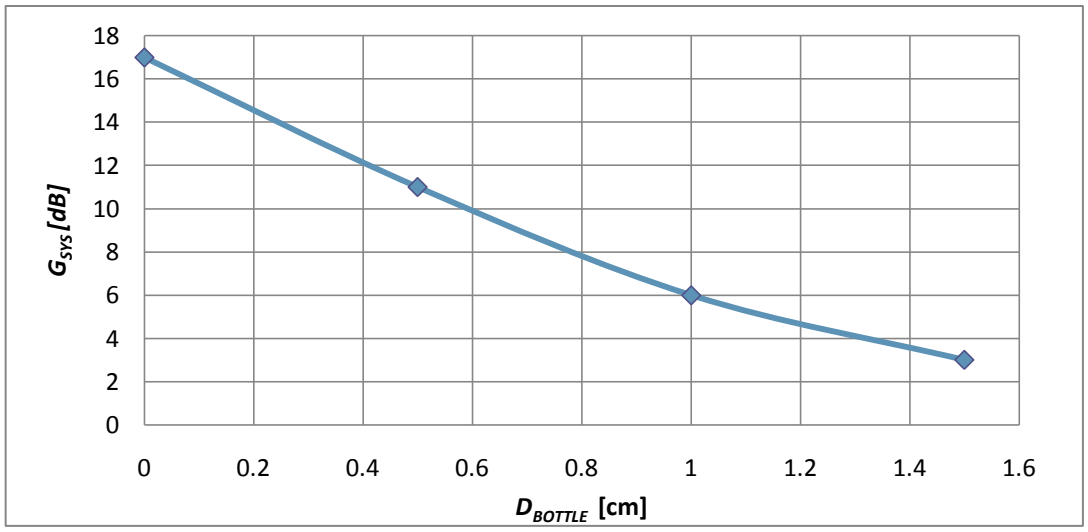

Figure 35: Gain provided by the system versus the distance from the bottle to the antenna

As it was said before, in this experiment was also computed the gain that the global system provided. If the obtained data and *Figure 35* are analyzed, one can conclude that the algorithm gain is better when the body effect is stronger (the body is closer). This affirmation could be explained if the S_{11} curve of the mobile is observed. The closer the body is, the lower center frequency becomes, so the higher return losses are in the reference high frequency (419 MHz was the best frequency channel with no bottle in the experiment). Since the power decreases more quickly (see *Table 3*) along the $RSSI_{NA}$ column than along the $RSSI_{BEST}$ column, the experimented gain is higher when the object gets closer.

Finally, if *Figure 12* is looked again it can be noticed a possible mismatch between the center frequency of the PIFA antenna, which is around 430 MHz, and the best frequency channel found by the algorithm, which is 419 MHz. This frequency mismatching was attributed to various factors like closer objects inside the laboratory; the effect of the connector from the PCB to the computer; the degradation caused by the realized gain of the base station antenna (approximately 1 dB); and the fact that the mobile terminal stays at the first best frequency found, so at higher frequency channels, the RSSI could be equal or almost equal.

Another consequence of the mismatch just mentioned above is observed in the last two rows of *Table 3*: both contain the same CH_{BEST} (391 MHz). Theoretically the best frequency for 0 cm distance would be lower than for 0.5 cm, but the algorithm could not find it because the lower frequency at which the CC1110 can work is 391 MHz. However, that unknown best channel should not be too far away from 391 MHz frequency because the system still provides acceptable gain.

4.2. Experiments in the garage

The second experiment was carried out in the garage of the building. There, more space was available so longer range tests could be performed. Moreover, the distance between the antenna and the body was fixed then, and it was compared the effect of the before used water bottle and a real human hand.

Figure 36: Base station in the garage experiment

Figure 37: Mobile terminal and bottle in the garage experiment

Both devices were placed on a carton box, which was on a tripod, at the same height and connected to the computers to obtain the program results, as it was done before in the laboratory. *Figure 36*, *Figure 37* and *Figure 38* show the positions of the devices and the rest of elements that took part in the experiment.

Figure 38: Relative position of the bottle to the mobile terminal

The parameters which were used in this experiment were the same than the previously used inside the lab except the following:

- Distance between devices (*d*): 10 and 20 m approximately.
- Height of both devices (from the floor to the device): 1.25 m

- Transmitted power in both directions: 10 dBm (notice the difference with the laboratory experiment)
- Distance between the bottle/hand and the antenna: about 5 cm. Body placed between the base station and the mobile terminal.

Below, the values obtained for the best channel (CH_{BEST}) found by the algorithm and its corresponding RSSI ($RSSI_{BEST}$) are shown. It is worth looking at the variations when it was substituted the bottle for the hand, and those caused by the modification of the distance which separated the devices.

d	**Kind of body**	CH_{BEST}	f_{DIFF}	$RSSI_{BEST}$
10 m	Nothing	427 MHz	-	-37 dBm
	Bottle	411 MHz	16 MHz	-47 dBm
	Hand	423 MHz	4 MHz	-45 dBm
20 m	Nothing	417 MHz	-	-40 dBm
	Bottle	403 MHz	14 MHz	-50 dBm
	Hand	407 MHz	10 MHz	-43 dBm

Table 4: Results of the experiment in the garage

Some aspects can be discussed if *Table 4* is observed carefully. First of all, when there is no body affecting the mobile terminal antenna, the best channel found for 20 m separation (417 MHz) agrees with the one found in the laboratory experiment. However, for 10 m it exists a mismatching (427 MHz), which is possibly caused by different propagation conditions although, for a body presence, CH_{BEST} still goes down.

Furthermore, it can be noticed that the difference in terms of RSSI between nothing present and bottle present is higher than inside the laboratory (about 5 dB higher). This is because in the garage experiment, unlike the previous experiment, the objects had been situated on the propagation path of the radio wave, so losses due to absorption were higher.

If now one focuses only on the data shown in *Table 4*, for both distance cases, it can be concluded that the influence of the water bottle is heavier than the influence of the hand in terms of frequency displacement (the bottle moves the best channels to a lower frequency) and power. However, the variation of f_{DIFF} and $RSSI_{BEST}$ is more consistent in the case of the bottle that in the case of the hand. For instance, for 10 m and bottle case, f_{DIFF} is 16 MHz and for 20 m is 14 MHz, so the difference is the smallest possible, whereas in the hand case, the values are 4 and 10 MHz, respectively, so the variation is greater. The same goes for $RSSI_{BEST}$, even it happens, for the hand case, that the power is greater for 20 m (-43 dBm) than for 10 m (-45 dBm), which does not make too much sense. These differences are caused by the higher level of uncertainty that the human hand introduces

(there are various studies about it, one of them is **[12]**), and that is just why a water bottle was used.

The last aspect to analyze is the different $RSSI_{BEST}$ values for the two distances tested, in the stable cases (nothing and bottle). It can be observed that the power is reduced 3 dB in both cases when the separation is doubled (from 10 to 20 m). Theoretically, the power reduction when doubling the distance would have to be -6 dB, but in this case power is reflected in the floor or in the walls. Consequently, the direct wave and the reflected waves were added constructively in this specific situation, thus causing that the power detect was higher than the one that is derived from the transmission equation. If packets had been employed in the system, the reflected waves could have caused ISI and, hence, errors in the demodulated bits.

Since for the garage experiment the power received once the algorithm has ended its function is around -50 dBm for 20 m distance, either the distance between the two devices could be increased or the transmitted power could be decreased. It was no space available to test the maximum range when using the maximum power (10 dBm), but if considered a 6 dB loss when the distance is doubled, it had been achieved a range about 300 m using the maximum power available in the device and having the RSSI above the threshold (-80 dBm). By contrast, the transmitted power could have been decreased until -20 dBm if the maximum range permitted had been 20 m.

To sum up, for both experiments described, the trend is the same, that is to get a new best channel which is placed at lower frequencies, as it was expected. After being shown the results of such experiments and discussed them, in the following chapter, final conclusions, advantages, drawbacks and possible improvements regarding to the whole project are going to be exposed.

5. Final conclusions and evaluation

5.1. Conclusions

In this project, a global system to avoid, or at least minimize, the detuning effect of the human body proximity on the antennas in mobile communications has been developed. The system consists of an algorithm that only takes profit of the communication and the interaction between the two basic elements that compose a radio communication: the base station and the mobile terminal. The process also has included the design and the fabrication of the antenna of the base station, whose properties has been adapted to the demands of the problem.

Both designs, antenna design (physical level) and algorithm design (protocol level), have been optimized to face specific requirements. These were fixed by some factors, such as frequency band (short range and low power bands), characteristics of the mobile terminal antenna (PIFA antenna) and human body effects on it, the chip that was used (CC1110), the propagation conditions, and so on. Once the antenna and the algorithm were finished, the whole system was tested and subjected to various experiments in order to get results which could demonstrate that the system worked correctly. Those results were analyzed and reasoned.

After completing all the stages, it is time to draw some conclusions. First of all, as some scientific studies (see *1.2.2*) say, it has been corroborated, trough direct measurements, that the human body affects significantly to the return loss characteristic of the antenna, displacing the center frequency to lower bands. In the case that the antenna occupy a small volume, like the mobile antenna terminal of this project, the effects could produce considerable degradation of the power received because of the increase of the reflection coefficient at the operating frequency.

Experimentally, the system has allowed measuring the amount of power loss by the effect of the human body effect. In general terms, the algorithm corrects the operating frequency of the communication elements and moves it to get the higher received power in the mobile terminal. This new frequency should be close to the frequency at which the center frequency of the antenna has been moved. From the parameters got at the end of the algorithm experiments, a loss around 11 dB (if 0.5 cm of body distance and 400 MHz band) was registered. It was seen that the loss became stronger when the body got closer to the antenna because of the combination of the detuning effect and the body absorption effect. Anyway, the system was able to provide considerable improvements in terms of received power.

Another important issue is that the system can reach its goal in a short time, which is a requirement for the current market devices. The quickest configuration tested were 600 ms, even though shorter time would have been achieved if the time to change the operating frequency or the number of frequencies to analyze had been reduced. On the

other hand, longer execution time could provide more accuracy when finding the adequate channel.

In addition to the conclusions just exposed, it is worth to summarize three more points, among others, which have been dealt with in this project. Firstly, all the surrounding elements of the communication scenario, not only the body near the antenna, modify the antenna performance, so the results of the experiments for different environments do vary. As the algorithm always reaches the channel at which the power is higher, all the factors that influence or degrade the transmitted signal are already taken into account by the system.

Secondly, the trade-off between transmitted power and range can make the system more flexible. If the maximum power available and allowed (ISM bands) is employed the system could reach around 300 m theoretically in an almost free-obstacles scenario. If less power is transmitted, to avoid interfere other communications, it could be reached, for instance, approximately 20 m by only transmitting -20 dBm, also if there is no obstacles between the two devices. Obviously, in a more cluttered scenario the maximum range is reduced depending on the intensity of such clutter.

Lastly, since getting feasible and consistent measurements using real human hands is difficult it was necessary to use a substitute. A simple bottle of water was chosen because the human tissues are made up mostly of water. Then, the measurements were more precise and it was possible also to quantify exactly the distance that separated the body and the antenna during the experiments, despite the stronger effect of the bottle.

5.2. Advantages

The first advantage of the designed system that one can think is that is simple. The system is simple because does not require variable elements or networks (such as varactors) that changes the impedance of the mobile terminal antenna, but only requires the implementation of software. It is also simple, because does not demand the use of packets in the communication process between base station and mobile terminal. This can also be considered as a drawback as is said later. Apart from making the system simpler, the omission of packets can increase the speed of the algorithm because less processing time is needed.

Moreover, if it is supposed that the band at which the system operates (remember, 391 – 431 MHz) is not too much occupied in terms of time, the probability of interfering other devices is very low because the transmitting time in each channel is quite short (10, 25 or 50 ms). Besides, this probability is low because the devices never go to the transmit mode if they detects that a signal already exist at the operating frequency.

Finally, since the algorithm takes decisions based on the power received, which is under the effects not only of the human body, but all the objects that reflect and absorb the propagated wave, the system can work as a real time adaptive mechanism which always establishes communication trough the best possible channel.

5.3. Drawbacks

If the previous advantages are analyzed from another point of view, they can be considered as disadvantages under certain circumstances. For example, in the case that the protocol had implemented packets, some interference situations could have been avoided since the base station and the terminal only would have worked if the identification, which can be read from the packets, was valid. Furthermore, even though with the designed algorithm both communication elements always are synchronized, the base station does not have all the information obtained by the mobile terminal (e.g. power of the different channels tested), which could be useful to provide more intelligence to the system. Packets could have carried this information.

Another drawback is the interference that can cause and suffer the system. If the bandwidth is utilized by a large number of devices, the amount of channels which are free decreases and the probability of causing interference raises. Therefore, more precision would be required for the implemented algorithm (i.e. reducing the frequency step), thus making longer the execution time. On the other hand, other sources working within the same frequency bandwidth could produce a non-desired start or stop of the algorithm. A way to avoid interferences in general is to restrict either the transmitted power or the system range.

5.4. Possible improvements

The most improvements that could be carried out in the designed algorithm are related to the disadvantages just exposed above. As is commented before, packets would provide extra intelligence to the whole system as well as a wide quantity of new possibilities. One of them could be the chance of extend the system to a multi-user scenario, that is one base station and more than one mobile terminal. The identification made possible by the transmission of packets would facilitate the calibration, in case of human body effect, for each device at different moments (TDMA).

In addition, the use of packets would make that the system of this project was something more than a simple frequency correction protocol. The base station, could record all the data provided by the different mobile terminals in different scenarios and when the base station found matching conditions (i.e. power similar for the most of the channels), all the devices would be able to update their parameters (timing, channelization, power, etc.) in order to optimize the system performance in such specific environment.

Acknowledgments

I am very grateful to all the mates from the Tsinghua University Antenna and Microwaves Laboratory for their practical help. Especially I would like to thank the student Xiaoye Sun who let me use his designs in my project and was extremely helpful. I also really appreciate the support of Professor Zhijung Zhang as well as his constant interest in my work.

Thanks to Tsinghua University for accepting me as an exchange student and thanks to my home university Universitat Politècnica de Catalunya for giving me the chance of going to China to perform my degree project.

Finally, I want to dedicate this project to my mother, my father, my brother, my whole family and my friends because I love them.

Bibliography

General bibliography

- C. A. Balanis, "Antenna Theory: Analysis and Design", Ed. John Wiley & Sons, 2005
- J.R. James, K. Fujimoto, "Mobile Antenna Systems Handbook", Ed. Artech House, 2008
- Z. N. Chen, "Antennas for Portable Devices", Ed. John Wiley & Sons, 2007

Specific references

[1] Q. Balzano, J. Irwin, and R. Steel, "Investigation of the impedance variation and radiation loss in portable radios," in *Proc. Antennas and Propagation Society Int. Symp.*, Jun. 1975, vol. 13, pp. 89-92.

[2] J. Toftgard, S. N. Hornsleth, and J. B. Andersen, "Effects on Portable Antennas of the Presence of a Person," *IEEE Trans. Antennas Propag.*, vol. 41, no. 6, pp. 739-746, Jun. 1993.

[3] G. F. Pedersen, K. Olesen, and S. L. Larsen, "Bodyloss for handheld phones," in *Proc. IEEE 49th Vehicular Technology Conf.,* 1999, vol. 2, pp. 1580-1584.

[4] K. R. Boyle, "The Performance of GSM 900 Antennas in the Presence of People and Phantoms," in *Proc. 12th Int. Conf. Antennas and Propagation (ICAP 2003),* Exeter, U.K. Mar. 31-Apr. 3 2003, vol. 1, pp. 35-38.

[5] K.R. Boyle, Yun Yuan, and L. P. Ligthart, "Analysis of Mobile Phone Antenna Impedance Variations With User Proximity," *IEEE Trans. Antennas Propag.*, vol. 55, no. 2, pp. 364-372, Feb. 2007.

[6] Y. Sun and J. K. Fidler, "High-speed automatic antenna tuning units," in *Proc. 9th Int. Conf. Antennas and Propagation, ICAP'95*, Apr. 1995, vol. 1, no. 4–7, pp. 218–222.

[7] I. Ida, J. Takada, T. Toda, and Y. Oishi, "An adaptive impedance matching system and considerations for a better performance," in *Proc. Joint Conf. 10th Asia-Pacific Conf. Communications 2004 and 5th Int. Symp. on Multi-Dimensional Mobile Communications*, Aug.–1 Sep. 2004, vol. 2, no. 29, pp. 563–567.

[8] J. de Mingo, A. Valdovinos, A. Crespo, D. Navarro, and P. Garcia, "An RF electronically controlled impedance tuning network design and its application to an antenna input impedance automatic matching system," *IEEE Trans. Microw. Theory Techniques*, vol. 52, no. 2, pp. 489–497, Feb. 2004.

[9] P. M. Evjen, "Application Note AN001: SRD Regulations for license free transceiver operation", http://focus.ti.com/lit/an/swra090/swra090.pdf, Chipcon Products from Texas Instruments.

[10] "True System-on-Chip with Low Power RF Transceiver and 8051 MCU (Rev. F)", focus.ti.com/lit/ds/swrs033g/swrs033g.pdf, Texas Instruments.

[11] R. Morrow, "Wireless network coexistence", Ed. McGraw-Hill, 2004, pp. 88.

[12] J. Krogerus, C. Icheln, P. Vainikainen, "Effect of the Human Body on Total Radiated Power and the 3-D Radiation Pattern of Mobile Handsets", *Instrumentation and Measurement, IEEE Trans. On,* vol. 56, no. 6, pp. 2375 - 2385, Dec. 2007.

Appendix A: Mobile terminal antenna parameters

The design and fabrication of both PCBs used along the project had been carried out by Xiaoye Sun, a student from Tsinghua University. The PCBs include the chip CC1110, capacitors, inductors, LEDs and other electronic elements conveniently placed and connected. The dimensions of the base station PCB (see *3.1*) are smaller than the dimensions of the mobile terminal PCB because on this second board was printed an antenna.

The designed antenna is a PIFA and is placed on the top of the PCB. It consists of a meandered line of metal printed on a FR-4 substrate. It has the appropriate length to provide resonance around 400 MHz. *Figure 39* shows the aspect of the whole mobile terminal PCB as well as the designed PIFA, and *Table 5* presents the dimensions corresponding to the parameters of *Figure 39*. It has to be noticed that there is a series capacitor incorporated in the antenna design that can control the S_{11} (hence, the center frequency) curve of the antenna as is going to be seen later.

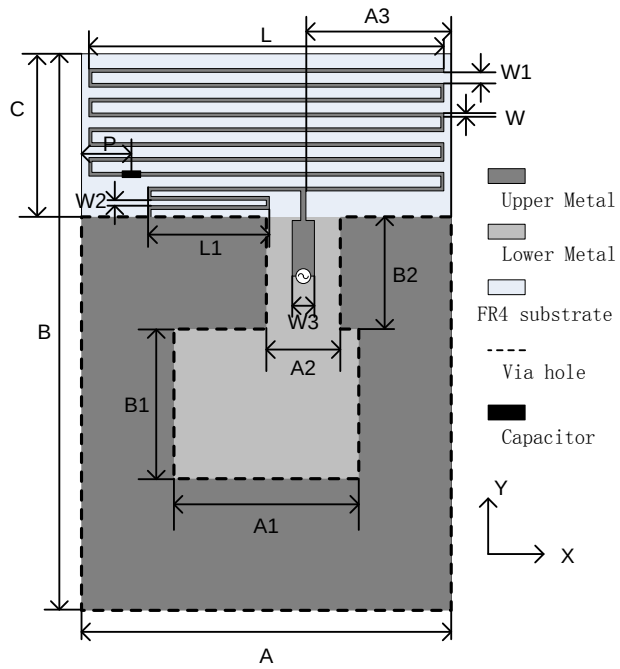

Figure 39: **Mobile terminal and its antenna sketch**

A	50	**A1**	30	**A2**	9	**A3**	10.25
B	80	**B1**	20	**B2**	15	**C**	20
L	48	**L1**	19.5	**W**	0.5	**W1**	1.6
W2	0.67	**P**	5				

Table 5: **Parameters and dimensions (mm) of *Figure 39***

The S_{11} reflection coefficient was simulated and plotted for different values of the aforementioned capacitor and the results are shown in *Figure 40*. It can be observed that the higher value of the capacitor, the lower center frequency of the antenna. The S_{11} of the antenna utilized in this project was measured and was found that the actual center frequency was around 430 MHz. However, if one looks at the simulated plot of S_{11}, none of the values provide that center frequency and the actual value was unknown even for the designer.

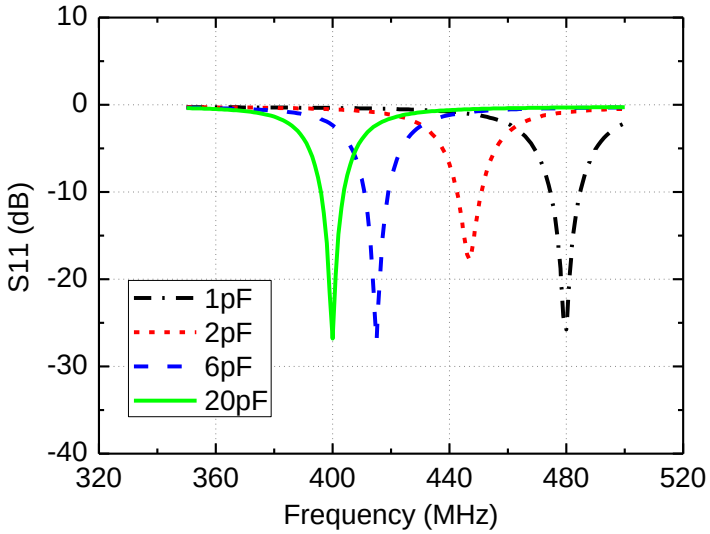

Figure 40: Reflection coefficient for different values of the series capacitor

If the tendency of the curves is observed, only can be intuited that the capacitor value used had to be between 2 and 6 pF. This suspicious was confirmed when the value was measured in the laboratory (with the Philips PM 6303 RLC Meter) and was proved that the actual value was 2.8 pF. The fact that the value of the capacitor could control the center frequency was useful to the student who designed the PCB because his project consisted of, unlike the present project, compensation of the human body effect trough variable capacitors (i.e. varactors).

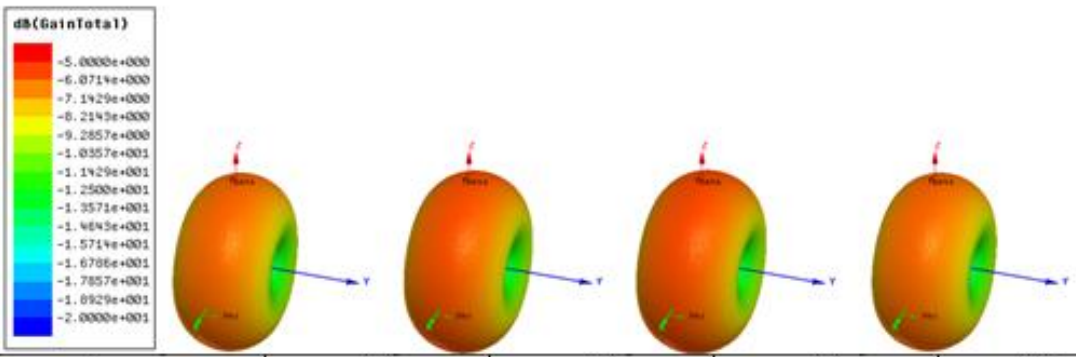

No.	(a)	(b)	(c)	(d)
Capacitor (pF)	20	6	2	1
Frequency (MHz)	400	415	447	480

Figure 41: Radiation pattern of the PIFA for different capacitor values

Regarding the radiation pattern of the PIFA designed, it has to be said that has an omnidirectional pattern, as is expected for this kind of devices. In *Figure 41* this pattern can be observed and how it remains unalterable when the series capacitor varies. It is important to notice that the gain at the center frequency is around -6 dB, hence it is very low. There is a reason that can explain this: the substrate that supports the antenna element is a dielectric (FR-4) that introduces high losses, thus decreasing the gain.

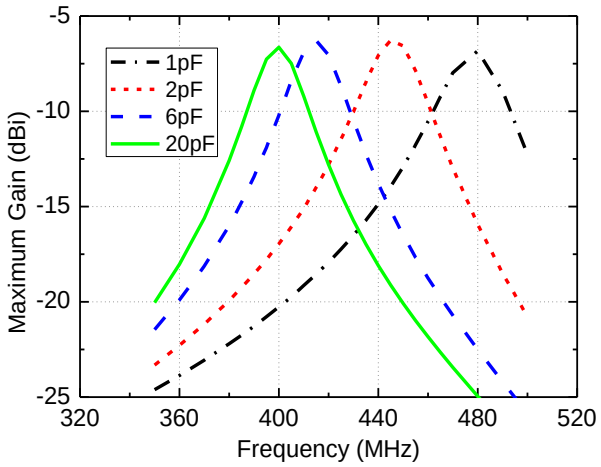

Figure 42: Simulation of the realized gain of the PIFA antenna for different capacitor values

Moreover, it was also simulated and plotted the realized gain of the antenna for different values of the series capacitor (see *Figure 42*). It is interesting to see that for those curves close to 430 MHz, the realized gain is around -10 dB at the frequency that is separated 20 MHz from the center frequency. This value was used at the end of *3.1.2* for a theoretical calculation.

Finally, the designer of the mobile terminal device performed some measurements (for 2 pF value of the capacitor) to know how the S_{11} parameter is affected when a bottle plenty of water is near the antenna. In *Figure 43* it can be observed that the center frequency is displaced to lower frequencies, as has been verified along the present project.

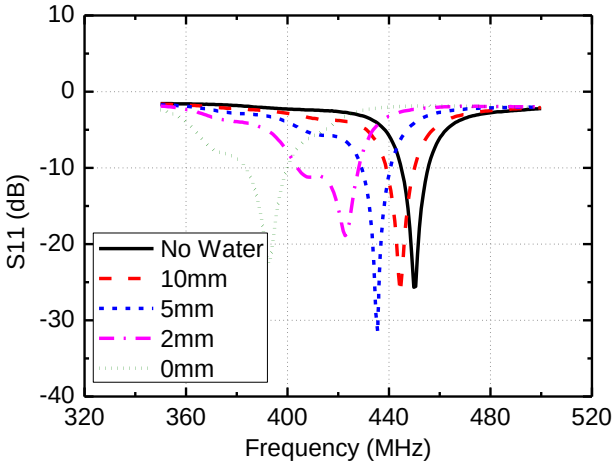

Figure 43: Effect of the water bottle on the antenna reflection coefficient when the capacitor value is 2 pF

Appendix B: SmartRF Studio 7

SmartRF Studio 7 is a software application that allows designers to handle the RF functions of the CC1110 System-on-Chip, among others, for testing purposes. Once the device is connected to the computer, trough the USB port, where SmartRF Studio is installed and it recognizes the device, one can start the configuration.

Inside the SmartRF Studio interface (see *Figure 44*), all the radio parameters (such as base frequency, channel, modulation, data rate, deviation, channel spacing, receiving filter bandwidth, transmitted power, synchronism word and preambles for packets, etc.) can be modified. When these parameters are introduced in the interface, the application automatically update the corresponding RF registers of the CC1110. The resultant configuration can be exported easily to several formats, including a format suitable for C code.

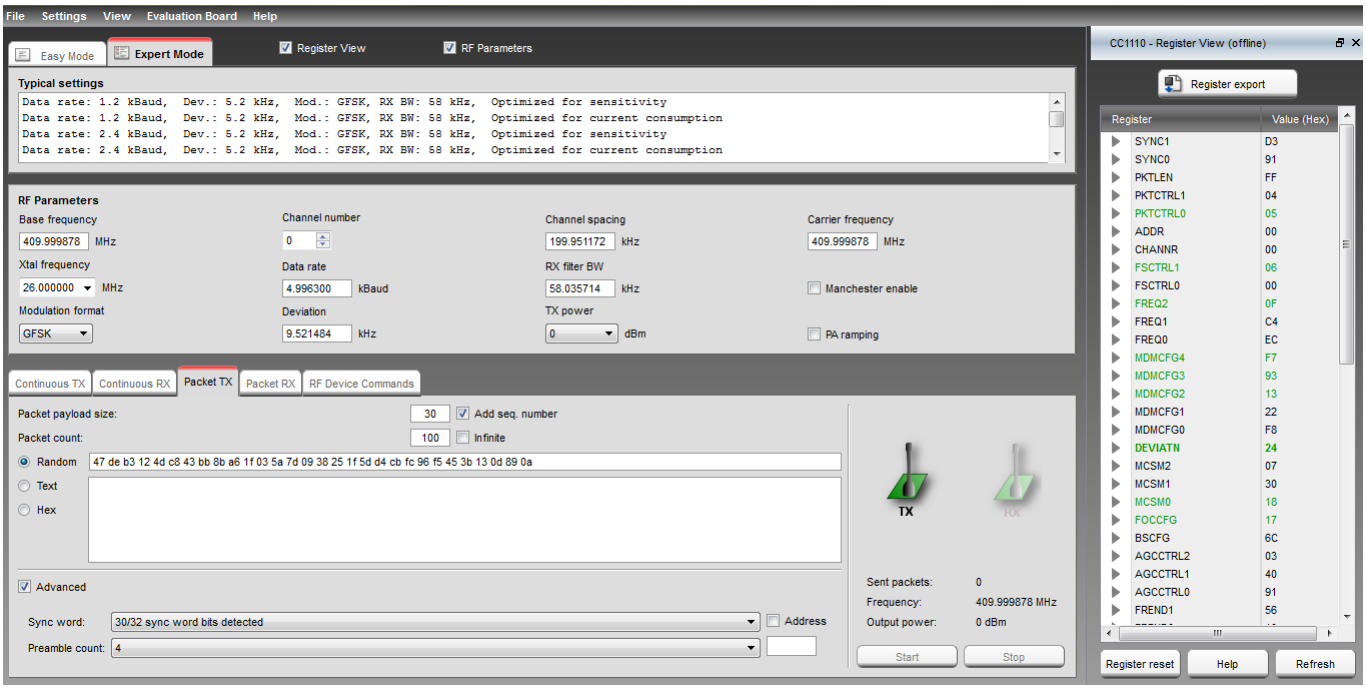

Figure 44: SmartRF Studio 7 interface

Besides the support for the radio registers settings, SmartRF Studio makes the test of a specific configuration possible. There are available up to five modes: Continuous TX, Continuous RX, Packet TX, Packet RX and RF Device Commands. The function of the two first modes is to transmit and receive signal in order to make simple tests related to power level, modulation or frequency aspects. Concerning the two packet modes, they are used, for instance, to test different packet formats or see if a specific configuration provide an acceptable error rate under certain conditions defined by the designer. Finally, the last mode facilitates the interaction with the radio state machine of the CC1110.

All the utilities that SmartRF Studio provides were very helpful in the coding stage of the present project. While in one of the two devices, the program was being executed, in the other one, was checked that the different stages of the algorithm were reached correctly. In addition, SmartRF Studio was used to control one of the devices to interact at the appropriate moment, like it was actually executing the code, with the one which was being tested.

Appendix C: Program codes

Base station code

```
#include <ioCC1110.h>
#include "ioCCxx10_bitdef.h"
#define BIT0 0x01
#define BIT1 0x02
#define BIT2 0x04
#define BIT3 0x08
#define BIT4 0x10
#define BIT5 0x20
#define BIT6 0x40
#define BIT7 0x80
#define P500 1 //sweep freq period
#define P250 2
#define P50 3
#define P25 4
#define P10 5
#define STEP 10 //sweep step, 10=>2MHz
#define SWEEP 0
#define COMMRX 1
#define COMMTX 2
#define ENDTX 3
#define ENDRX 4
#define TH -80

static unsigned int best_channel_test;
static unsigned char current_channel;
static unsigned char state;
static int rssi;
static int rssi_old;
static int tick;
static int ntick1; //controls the listening time
static int ntick2; //controls the ack time

void startCommToMT();
void confTxCarrier();
int absRSSI();
void goToTx();
void goToRx();
void goToIdle();
void initSettings();
void reset();

#pragma vector = T1_VECTOR
__interrupt void timer1_ISR(void)
{
    T1CTL &= ~BIT5; //clear timer1 channel0 interrupt (CHOIF=0)

    P1_0 ^= 1; //toggle led

    goToIdle();

    startCommToMT(); //rx possible packet about best channel

    //if data received from mobile terminal, timer interrupts
(sweep) disabled
    if(state==SWEEP){
      goToIdle();

      if(CHANNR == 0xC8) //if upper frequency reached
        CHANNR = 0x00; //return
      else
         CHANNR+=STEP; //carrier frequency displaced one channel

       confTxCarrier(); //continue tx carrier
       goToTx();
```

```
    }

    current_channel=CHANNR;
}

#pragma vector = T3_VECTOR
__interrupt void timer3_ISR(void)
{
  T3IF=0;
  tick++; //1 tick = 2.5ms
  if(state==COMMRX){
    if(tick==ntick1){
      T3IE=0; //disable timer 3 interrupts
      T3CTL &= ~BIT4; //stop timer 3
      T3CTL |= BIT2; //reset timer 3
      IEN2 &= ~BIT0; //disable radio interrupts;
      tick=0;
      state=SWEEP; //timeout, continue sweepping
    }
  }else if(state==COMMTX){
    if(tick==ntick2){
      best_channel_test=CHANNR/STEP;
      state=ENDTX;
    }
  }
}

#pragma vector = T4_VECTOR
__interrupt void timer4_ISR(void)
{
  T4IF=0;
  tick++;
  if(tick==400){ //400=2seg
    T4IE=0; //disable timer 4 interrupts
    T4CTL &= ~BIT4; //stop timer 4
    T4CTL |= BIT2; //reset timer 4
    tick=0;
    if(state==ENDTX)
      state=ENDRX;
    else if(state==ENDRX)
      state=ENDTX;
  }
}

#pragma vector = RF_VECTOR
__interrupt void radio_ISR(void) //cs...
{
  RFIF &= ~BIT3; //clear carrier sense interrupt
  rssi=absRSSI(); //get power
  if(rssi>TH){ //signal power above treshold
      T1IE=0; //disable timer 1 interrupts
      T3IE=0; //disable timer 3 interrupts
      T3CTL &= ~BIT4; //stop timer 3
      T3CTL |= BIT2; //reset timer 3
      IEN2 &= ~BIT0; //disable radio interrupts;
      state=COMMTX;
  }
}

int absRSSI() //obtains RSSI in dBm
{
  unsigned char rssi_dec;
  int rssi_dBm;
  unsigned char rssi_offset = 75;
  rssi_dec = RSSI;
  if (rssi_dec >= 128)
    rssi_dBm = (int)((int)( rssi_dec - 256) / 2) - rssi_offset;
  else
  rssi_dBm = (rssi_dec / 2) - rssi_offset;

  return rssi_dBm;
}

void initRF()
{
  //data rate=5kbaud, dev=9.5kHz, RX filter BW=58kHz
  FSCTRL1   =     0x06; // Frequency Synthesizer Control
  FSCTRL0   =     0x00; // Frequency Synthesizer Control
```

```
FREQ2     =     0x0F; // Frequency Control Word, High Byte
FREQ1     =     0x09; // Frequency Control Word, Middle Byte
FREQ0     =     0xD8; // Frequency Control Word, Low Byte
MDMCFG4   =     0xF7; // Modem configuratio
MDMCFG3   =     0x93; // Modem Configuration
MDMCFG2   =     0x13; // Modem Configuration
MDMCFG1   =     0x22; // Modem Configuration
MDMCFG0   =     0xF8; // Modem Configuration
CHANNR    =     0x00; // Channel Number
DEVIATN   =     0x24; // Modem Deviation Setting
FREND1    =     0x56; // Front End RX Configuration
FREND0    =     0x10; // Front End TX Configuration
MCSM0     =     0x18; // Main Radio Control State Machine
FOCCFG    =     0x17; // Frequency Offset Compensation
BSCFG     =     0x6C; // Bit Synchronization Configuration
AGCCTRL2  =     0x3F; // AGC Control
AGCCTRL1  =     0x40; // AGC Control
AGCCTRL0  =     0x91; // AGC Control
FSCAL3    =     0xE9; // Frequency Synthesizer Calibration
FSCAL2    =     0x2A; // Frequency Synthesizer Calibration
FSCAL1    =     0x00; // Frequency Synthesizer Calibration
FSCAL0    =     0x1F; // Frequency Synthesizer Calibration
TEST2     =     0x88; // Various Test Settings
TEST1     =     0x31; // Various Test Settings
TEST0     =     0x0B; // Various Test Settings
PA_TABLE0 =     0x60; // PA Power Setting 0
PKTCTRL1  =     0x00; // Packet Automation Control
PKTCTRL0  =     0x22; // Packet Automation Control
ADDR      =     0x00; // Device Address
PKTLEN    =     0xFF; // Packet Length

SYNC1     = 0xD3;
SYNC0     = 0x91;

IP0=0x01;//Priority: Timer3, Radio, Timer1
IP1=0x08;

current_channel=CHANNR;
```

```
  RFIF =0x00; //clear all radio interrupt flags
  RFIM = BIT3; //enable only carrier sense interrupt
}

void initCLK ()
{
  SLEEP &= ~0x04; //both oscillators powered up
  while( !(SLEEP & 0x40) ); //wait for stable crystal
  CLKCON = 0x88; //CLKSPD=fref=26M, TICKSPD=fref/2=13M
  SLEEP |= 0x04; //only crystal ocillator selected
}

void initTimer (int speed)
{
  /*setup interrupt*/
  T1CTL &= ~BIT5; //clear timer1 channel0 interrupt (CHOIF=0)
  T1CCTL0 |= BIT6; //enable interrupt on channel 0
  T1CCTL1 &= ~BIT6; //disable interrupt on channel 1
  T1CCTL2 &= ~BIT6; //disable interrupt on channel 2
  OVFIM = 0; // Disable overflow interrupt

  T1IE=1; //enable timer1 interrupt (IEN1.T1IE=1)

  T1CCTL0 = 0x54; //Timer1 control configuration: normal input,
int enabled, toogle on compare, compare mode, no capture

  switch(speed){
  case P500: //not used
    T1CC0L = 0x2E;
    T1CC0H = 0x63;
  break;
  case P250: //not used
    T1CC0L = 0x97;
    T1CC0H = 0x31;
    ntick1=50;ntick2=400;
  break;
  case P50:
    T1CC0L = 0xEB;
    T1CC0H = 0x09;
```

```
    ntick1=10;ntick2=80;
  break;
  case P25:
    T1CC0L = 0xF6;
    T1CC0H = 0x04;
    ntick1=5;ntick2=40;
  break;
  case P10:
    T1CC0L = 0xFC;
    T1CC0H = 0x01;
    ntick1=2; ntick2=20;
  break;
  }

  T1CTL |= 0x0F; //up/down, tickspd/128

  T3CTL = 0xEA; // /128, modulo mode, no start, overflow interrupt
enabled
  T3CCTL0 = 0x00;
  T3CCTL1 = 0x00;
  T3CC0 = 0xFF; //interrupt period=2.5ms
  T4CTL = 0xEA; // /128, modulo mode, no start, overflow interrupt
enabled
  T4CCTL0 = 0x00;
  T4CCTL1 = 0x00;
  T4CC0 = 0xFF; //interrupt period=2.5ms
  T3IE=0;
  T4IE=0;

}

void goToTx(){
  RFST = 0x03; //enable tx
  while((MARCSTATE & MARCSTATE_MARC_STATE) != 0x13); //wait for
radio to enter in tx
}

void goToRx(){
  RFST = 0x02; //goto rx
  while((MARCSTATE & MARCSTATE_MARC_STATE) != 0x0D); //wait for
radio to enter in rx
}

void goToIdle(){
  RFST = 0x04; //go to idle
  while((MARCSTATE & MARCSTATE_MARC_STATE) != 0x01); //wait for
radio to enter in idle
}

void confRxCarrier ()
{
  /*register conf for Rx mode*/
  PKTCTRL0  = 0x00;
  PKTCTRL1  = 0x00;
  TEST2 = 0x81;
  TEST1 = 0x35;

}

void confTxCarrier ()
{
  /*register conf for Tx mode*/
  PKTCTRL0  = 0x22;
  PKTCTRL1  = 0x00;
  TEST2 = 0x88;
  TEST1 = 0x31;
}

void startCommToMT ()
{
  state=COMMRX;
  confRxCarrier();
  goToRx();

  T3IE=1; //enable timer 3 interrupt
  T3CTL |= BIT4; //start timer 3
  IEN2 |= 0x01; //enable radio interrupts, carrier sense interrupt
```

```
  while(state==COMMRX);

  if(state==COMMTX){
    goToIdle();

    confTxCarrier();
    goToTx();

    T3IE=1; //enable timer 3 interrupt
    T3CTL |= BIT4; //start timer 3

    while(state==COMMTX);
  }
}

void initSettings(){
    //base station chip: leds P1_0 and P1_1
  P1SEL &= ~0x03; //set P0 (led) as general purpose pin
  P1=0x00;//turn off leds
  P1DIR |= 0x03; //set P0 as output
  P1_0=1; //set leds outputs
  P1_1=1;

  initCLK(); //initialize clock
  initTimer(P25); //initialize timers choosing the sweep period
  initRF(); //initialize radio module

  goToTx();
  P0 = 0x01; //turn on led;

  EA=1; //enable global interrupt
}

void reset(){
   EA=0; //disable interrupts
   WDCTL = 0x03; //minimum period for WD
   WDCTL |= BIT3; //enable WD
   while(1); //wait for reset, so go to WAIT
}
```

```
int main (void)
{
  initSettings();

  while(state!=ENDTX);
  //best channel found and comm started
  while(1){
    //TX MODE
    P1_1=0; //leds output
    P1_0=0;
    T3IE=0; //disable timer 3 interrupt
    T4IE=1; //enable timer 4 interrupt
    T4CTL |= BIT4; //start timer
    while(state==ENDTX); //wait for tx carrier
    //RX MODE
    P1_1=1; //leds output
    P1_0=1;
    goToIdle();
    confRxCarrier();//goto Rx mode
    goToRx();
    T4IE=1; //enable timer 4 interrupt
    T4CTL |= BIT4; //start timer 4
    rssi_old=absRSSI(); //get poer
    while(state==ENDRX){ //get the best power sample
      rssi=absRSSI();
      if(rssi>rssi_old)
        rssi_old=rssi;
    }
    if(rssi<TH){ //no rx carrier, so restart
      reset();
    }
    goToIdle();
    confTxCarrier();
    goToTx();
  }
}
```

Mobile terminal code

```
#include <ioCC1110.h>
#include "ioCCxx10_bitdef.h"
#define BIT0 0x01
#define BIT1 0x02
#define BIT2 0x04
#define BIT3 0x08
#define BIT4 0x10
#define BIT5 0x20
#define BIT6 0x40
#define BIT7 0x80
#define P500 1
#define P250 2
#define P50 3
#define P25 4
#define P10 5
#define STEP 10 //sweep step, 10->2 MHz
#define WAIT 0
#define SWEEP 1
#define ROUND 2
#define COMMTX 3
#define COMMRX 4
#define ENDRX 5
#define ENDTX 6
#define TH -80

static int q; //power in dBm to measure the link quality
static int rssi_test;
static unsigned char initial_channel;
static unsigned char best_channel;
static unsigned char test_current_channel;
static unsigned int best_channel_test;
static char state;
static int tick; //control the tx/rx time in states 3 and 4
static int power [50]; //array where store new best channels
static int count;
static int ntick;

void initTimer();
int absRSSI();
void testChannel();
void startCommToBS ();
void goToTx();
void goToRx();
void goToIdle();
void initSettings();
void reset();

#pragma vector = T1_VECTOR
__interrupt void timer1_ISR(void)
{
  T1CTL &= ~BIT5; //clear timer1 channel0 interrupt (CHOIF=0)

  P1_0=1; //turn off led
  if (P0==0x00)
     P0=0x01;
  else
    P0 <<= 1;

  if(state==ROUND && CHANNR == best_channel){
    T1IE=0; //disable timer1 interrupt (IEN1.T1IE=0)
    state=COMMTX;
  }

  if(state == SWEEP || state==ROUND){
    goToIdle();

    if(CHANNR == 0xC8) //if bandwith sweep completed
      CHANNR = 0x00; //return to first freq*/
    else
      CHANNR+=STEP;
    if(state == SWEEP){
      if(CHANNR==initial_channel) //if CH0 reached
        state=ROUND; //one round complete, no more power checking
```

```
      goToRx();
    }

  }

  test_current_channel=CHANNR;
}

#pragma vector = T3_VECTOR
__interrupt void timer3_ISR(void)
{
  T3IF=0; //clear interrupt
  tick++; //1 tick=2.5ms
  if(tick==ntick){
    T3IE=0; //disable timer 3 interrupts
    T3CTL &= ~BIT4; //stop timer 3
    T3CTL |= BIT2; //reset timer 3
    tick=0;
    if(state==COMMTX)
      state=COMMRX;
    else if(state==COMMRX){ //no ack received, timeout
      reset();
    }
  }
}
#pragma vector = T4_VECTOR
__interrupt void timer4_ISR(void)
{
  T4IF=0; //clear interrupt
  tick++;
  if(tick==400){ //400=2seg
    T4IE=0; //disable timer 4 interrupts
    T4CTL &= ~BIT4; //stop timer 4
    T4CTL |= BIT2; //reset timer 4
    tick=0;
    if(state==ENDTX)
      state=ENDRX;
    else if(state==ENDRX)
      state=ENDTX;
  }
}

#pragma vector = RF_VECTOR
__interrupt void radio_ISR(void) //cs...
{
  RFIF &= ~BIT3; //clear carrier sense interrupt
  q=absRSSI(); //get power
  if(q>TH){ //carrier condition
    switch(state){
    case WAIT:
      IEN2 &= ~BIT0; //disable radio interrupt
      T1IE=1; //enable timer1 interrupt
      T1CTL |= 0x0F; //up/down, tickspd/128, start timer1
      testChannel();
    break;
    case COMMRX: //ack from BS received
        T3IE=0; //disable timer 3 interrupts
        IEN2 &= ~BIT0; //disable radio interrupt
        state=ENDRX;
    break;
    }
  }
}


void testChannel()
{
  if(state==WAIT){
    state=SWEEP;
    P1_0=0; //turn on detection LED
    power[count]=q; //store sample
  }else{
    if(rssi_test>q){ //find the best power sample
      P1_0=0; //turn on detection white LED
      q=rssi_test;
      power[count]=q; //store sample
      count++;
```

```
      best_channel=CHANNR; //at the moment, the best channel is
the current channel
    }
  }
}

int absRSSI() //obtains RSSI in dBm
{
  unsigned char rssi_dec;
  int rssi_dBm;
  unsigned char rssi_offset = 75;
  rssi_dec = RSSI;
  if (rssi_dec >= 128)
    rssi_dBm = (int)((int)( rssi_dec - 256) / 2) - rssi_offset;
  else
  rssi_dBm = (rssi_dec / 2) - rssi_offset;

  return rssi_dBm;
}
void initRF()
{
//data rate=5kbaud, dev=9.5kHz, RX filter BW=58kHz
FSCTRL1    =     0x06; // Frequency Synthesizer Control
FSCTRL0    =     0x00; // Frequency Synthesizer Control
FREQ2      =     0x0F; // Frequency Control Word, High Byte
FREQ1      =     0x09; // Frequency Control Word, Middle Byte
FREQ0      =     0xD8; // Frequency Control Word, Low Byte
MDMCFG4    =     0xF7; // Modem configuration
MDMCFG3    =     0x93; // Modem Configuration
MDMCFG2    =     0x13; // Modem Configuration
MDMCFG1    =     0x22; // Modem Configuration
MDMCFG0    =     0xF8; // Modem Configuration
CHANNR     =     0x1A; // Channel Number
DEVIATN    =     0x24; // Modem Deviation Setting
FREND1     =     0x56; // Front End RX Configuration
FREND0     =     0x10; // Front End TX Configuration
MCSM0      =     0x18; // Main Radio Control State Machine
FOCCFG     =     0x17; // Frequency Offset Compensation
BSCFG      =     0x6C; // Bit Synchronization Configuration
AGCCTRL2   =     0x03; // AGC Control
AGCCTRL1   =     0x40; // AGC Control
AGCCTRL0   =     0x91; // AGC Control
FSCAL3     =     0xE9; // Frequency Synthesizer Calibration
FSCAL2     =     0x2A; // Frequency Synthesizer Calibration
FSCAL1     =     0x00; // Frequency Synthesizer Calibration
FSCAL0     =     0x1F; // Frequency Synthesizer Calibration
TEST2      =     0x81; // Various Test Settings
TEST1      =     0x35; // Various Test Settings
TEST0      =     0x0B; // Various Test Settings
PA_TABLE0  =     0x60; // PA Power Setting 0
PKTCTRL1   =     0x00; // Packet Automation Control
PKTCTRL0   =     0x00; // Packet Automation Control
ADDR       =     0x00; // Device Address
PKTLEN     =     0xFF;  // Packet Length

SYNC1      = 0xD3;
SYNC0      = 0x91;

if(CHANNR % STEP!=0)//if the channel is not a multiple of the
sweep step
  CHANNR = (CHANNR/STEP)*STEP;

initial_channel=test_current_channel=best_channel=CHANNR;

IP0=0x01; //Priority: Timer3, Radio, Timer1
IP1=0x08;
  /*setup radio general interrupt*/
RFIF =0x00; //clear all radio interrupt flags
RFIM = BIT3; //enable only carrier sense interrupt
}

void initCLK()
{
  SLEEP &= ~0x04; //both oscillators powered up
  while( !(SLEEP & 0x40) ); //wait for stable crystal
  CLKCON = 0x88; //CLKSPD=fref=26M, TICKSPD=fref/2=13M
  SLEEP |= 0x04; //only crystal ocillator selected
}
```

```
void initTimer (int speed)
{
  /*setup interrupt*/
  T1CNTL=0x00;
  T1CTL &= ~BIT5; //clear timer1 channel0 interrupt (CHOIF=0)
  T1CCTL0 |= BIT6; //enable interrupt on channel 0
  T1CCTL1 &= ~BIT6; //disable interrupt on channel 1
  T1CCTL2 &= ~BIT6; //disable interrupt on channel 2
  OVFIM = 0; // Disable overflow interrupt

  T1CCTL0 = 0x54; //Timer1 control configuration: normal input,
int enabled, toogle on compare, compare mode, no capture

  switch(speed){
  case P500: //not used
    T1CC0L = 0x2E;
    T1CC0H = 0x63;
  case P250: //not used
    T1CC0L = 0x97;
    T1CC0H = 0x31;
    ntick=2010;
  break;
  case P50:
    T1CC0L = 0xEB;
    T1CC0H = 0x09;
    ntick = 410;
  break;
  case P25:
    T1CC0L = 0xF6;
    T1CC0H = 0x04;
    ntick=210;
  break;
  case P10:
    T1CC0L = 0xFC;
    T1CC0H = 0x01;
    ntick=85;
  break;
  }
  T3CTL = 0xEA; //128, modulo mode, no start, overflow interrupt
  T3CCTL0 = 0x00;
  T3CCTL1 = 0x00;
  T3CC0 = 0xFF; //interrupt period=2.5ms
  T4CTL = 0xEA; // /128, modulo mode,no start,overflow interrupt
  T4CCTL0 = 0x00;
  T4CCTL1 = 0x00;
  T4CC0 = 0xFF; //interrupt period=2.5ms
  T3IE=0;
  T4IE=0;
}

void goToTx(){
  RFST = 0x03; //enable tx
  while((MARCSTATE & MARCSTATE_MARC_STATE) != 0x13);//wait for
radio to enter in tx

}

void goToRx(){
  RFST = 0x02; //goto rx
  while((MARCSTATE & MARCSTATE_MARC_STATE) != 0x0D); //wait for
radio to enter in rx
}

void confRxCarrier ()
{
  PKTCTRL0  = 0x00;
  PKTCTRL1  = 0x00;
  TEST2 = 0x81;
  TEST1 = 0x35;
}

void confTxCarrier ()
{
  PKTCTRL0  = 0x22;
  PKTCTRL1  = 0x00;
  TEST2 = 0x88;
```

```
  TEST1 = 0x31;
}

void goToIdle(){
  RFST = 0x04; //go to idle
  while((MARCSTATE & MARCSTATE_MARC_STATE) != 0x01); //wait for
radio to enter in idle
}

void startCommToBS ()
{
  goToIdle();
  confTxCarrier();
  goToTx();

  T3IE=1; //enable timer 3 interrupt
  T3CTL |= BIT4; //start timer 3

  while(state==COMMTX);//wait for tx carrier

  confRxCarrier();
  goToRx();

  T3IE=1; //enable timer 3 interrupt
  T3CTL |= BIT4; //start timer 3
  RFIF =0x00; //clear all radio interrupt flags
  RFIM = BIT3; //enable only carrier sense interrupt
  IEN2 |= 0x01; //enable radio interrupts, carrier sense interrupt

  while(state==COMMRX);//wait for ack
}

void initSettings(){
  state=WAIT;

  P0SEL &= ~0xFF; //set P0 (led) as general purpose pin
  P1SEL &= ~0x01; //set P1_0 as general purpose pin
  P0=0x00; P1_0=1; //turn off leds
  P1DIR |= 0x01; //set P1_0 as output
  P0DIR |= 0xFF; //set P0 as output

  count=tick=0;

  initCLK();
  initTimer(P25);
  initRF();

  goToRx();
  P0=0x01; ////turn on blue led (listening)

  IEN2 |= BIT0; //enable radio interrupts
  EA=1; //enable global interrupt
}

void reset(){
   EA=0; //disable interrupts
   WDCTL = 0x03; //minimum period for WD
   WDCTL |= BIT3; //enable WD
   while(1); //wait for reset, so go to WAIT
}

int main (void)
{
  initSettings();

  while(1){
    if(state==SWEEP){//sweep the BW getting power samples
      rssi_test=absRSSI();
      testChannel();
    }
    if(state==COMMTX)
      startCommToBS(); //notice the BS that best channel found
    if(state==ENDRX){
        best_channel_test=best_channel/STEP;
        while(1){
          //RX MODE
          P0=0xAA; //set led output
          T3IE=0; //disalbe timer 3 interrupt
```

```
          T4IE=1; //enable timer 4 interrupt
          T4CTL |= BIT4; //start timer
          q=absRSSI(); //get power sample

          while(state==ENDRX){ //timer4 will end this mode
            rssi_test=absRSSI();
            if(rssi_test>q)
              q=rssi_test;
          }

          if(q < (power[count-1]-5) || q > (power[count-
1]+5)){//if body effect
            reset(); //restart
          }else{ //no boddy effect, so goto Transmit mode
              P0=~0xAA;
              goToIdle();
              confTxCarrier();
              goToTx();
              T4IE=1; //enable timer 4 interrupt
              T4CTL |= BIT4; //start timer 4

              while(state==ENDTX);

              goToIdle();
              confRxCarrier();//goto Rx mode
              goToRx();
          }
        }
    }
  }
}
```